

# Four-Point Spectral Functions and Ward Identities in Hot QED

Hou Defu<sup>1,2,3</sup>, M.E. Carrington<sup>1,3</sup>, R. Kobes<sup>1,4</sup>, and U. Heinz<sup>5,\*</sup>

<sup>1</sup>Winnipeg Institute for Theoretical Physics, Winnipeg, Manitoba

<sup>2</sup>Institute of Particle Physics, Huazhong Normal University, 430070 Wuhan, China

<sup>3</sup>Physics Department, Brandon University, Brandon, Manitoba, R7A 6A9, Canada

<sup>4</sup>Physics Department, University of Winnipeg, Winnipeg, Manitoba, R3B 2E9, Canada

<sup>5</sup>Theoretical Physics Division, CERN, CH-1211 Geneva 23, Switzerland

(March 27, 2022)

We derive spectral representations for the different components of the 4-point function at finite temperature in the real time formalism in terms of five real spectral densities. We explicitly calculate all these functions in QED in the hard thermal loop approximation. The Ward identities obeyed by the 1-loop 3- and 4-point functions in real time and their spectral functions are derived. We compare our results with those derived previously in the imaginary-time formalism for retarded functions in hot QCD, and we discuss the generalization of our results to non-equilibrium situations.

PACS numbers: 11.10Wx, 11.15Tk, 11.55Fv

## I. INTRODUCTION

One of the most significant advances in quantum field theory at finite temperature [1–3] is the effective perturbation theory of Braaten and Pisarski [4,5] which is based on the resummation of hard thermal loops (HTLs). HTLs were originally obtained by computing one-loop diagrams in the imaginary time formulation of finite temperature field theory. HTLs are ultraviolet finite, gauge invariant and satisfy simple Ward identities [6–9]. These remarkable properties have been traced to the fact that HTLs describe simple semiclassical physics [6,10,11]. In particular, the HTLs can be derived from a set of classical kinetic equations [6,10] as well as from a non-local effective Lagrangian [8]. The computation of HTLs is fairly technical because of their non-trivial momentum and energy dependence, but can be simplified by using the Ward identities [4].

The analytical structure of Green functions at zero or non-zero temperature, in the imaginary or real-time formulations, is controlled by their spectral densities, combined with asymptotic boundary conditions. At finite temperature the spectral functions can also be directly related to transport coefficients [12,13]. The study of spectral functions helps us to understand the quasi-particle structure of a field theory and to identify the microscopic processes underlying the dynamics. But Green functions and their spectral functions are not easy quantities to evaluate perturbatively at non-zero temperature, especially for many-point functions. The two-point functions and their spectral densities have been widely studied and applied to quark gluon plasma (QGP) investigations [14,3,5,12]. Our knowledge about many-point spectral densities is still much less comprehensive [15–20]. The spectral representations of 3-point functions for self-interacting scalar fields were discussed in Refs. [15,16,19,20]. In [18] 3- and 4-point spectral densities for pure gluon dynamics were calculated in the HTL approximation using the imaginary time formalism (ITF) [4], and in the same approximation the 3-point spectral density in QED has been calculated within the real time formalism (RTF) [20].

The popularity of the RTF is diminished by the technical complications resulting from the doubling of degrees of freedom [21]. However, in the ITF, one has to perform an analytic continuation of the imaginary external energy variables to the real axis, which is avoided in the RTF. In addition, the ITF is restricted to equilibrium situations, while the RTF can be extended to investigate non-equilibrium systems [21–23].

In this paper we study 4-point functions in QED using the real-time formalism. We adopt the Keldysh or closed time path (CTP) contour [22]. In Sec. II we introduce the Keldysh representation. The spectral representations of the 4-point functions is derived in Sec. III. In Sec. IV we use the Keldysh representation to calculate the 4-point HTL vertex functions in hot QED. The 4-point spectral densities in the HTL approximation are extracted in Sec. V and shown to degenerate to a single real spectral function. In Sec. VI we derive real-time Ward identities between the 3-

---

\*On leave from Institut für Theoretische Physik, Universität Regensburg, D-93040 Regensburg, Germany.

and 4-point HTLs and their spectral functions. The generalization of our results to certain types of non-equilibrium situations is discussed in Sec. VII, while Sec. VIII gives a summary of our results.

## II. KELDYSH REPRESENTATION

We will use the Keldysh representation [21,22] of the real-time formalism (RTF) throughout this paper. In this representation the single-particle propagator for free bosons has in momentum space the form [21,22]

$$D(K) = \begin{pmatrix} \frac{1}{K^2 - m^2 + i\epsilon} & 0 \\ 0 & \frac{-1}{K^2 - m^2 - i\epsilon} \end{pmatrix} - 2\pi i \delta(K^2 - m^2) \begin{pmatrix} n_B(k_0) & \theta(-k_0) + n_B(k_0) \\ \theta(k_0) + n_B(k_0) & n_B(k_0) \end{pmatrix} \quad (1)$$

where  $K = (k_0, \mathbf{k})$ ,  $k = |\mathbf{k}|$ ,  $\theta$  denotes the step function, and the equilibrium distribution function is given by  $n_B(k_0) = 1/[\exp(|k_0|/T) - 1]$ . For fermions the bare propagator can be written as

$$S(K) = (\not{K} + m) \left[ \begin{pmatrix} \frac{1}{K^2 - m^2 + i\epsilon} & 0 \\ 0 & \frac{-1}{K^2 - m^2 - i\epsilon} \end{pmatrix} + 2\pi i \delta(K^2 - m^2) \begin{pmatrix} n_F(k_0) & -\theta(-k_0) + n_F(k_0) \\ \theta(k_0) - n_F(k_0) & n_F(k_0) \end{pmatrix} \right], \quad (2)$$

where the Fermi-Dirac distribution is given by  $n_F(k_0) = 1/[\exp(|k_0|/T) + 1]$ . The components of these propagators are not independent, but fulfill the relation

$$G_{11} - G_{12} - G_{21} + G_{22} = 0, \quad (3)$$

where  $G$  stands for  $D$  or  $S$ , respectively.

By an orthogonal transformation of these  $2 \times 2$  matrices one arrives at the representation of the propagators in terms of advanced and retarded propagators which was first introduced by Keldysh [22]. The three nonvanishing components of this representation are [21]

$$\begin{aligned} G_R &= G_{11} - G_{12}, \\ G_A &= G_{11} - G_{21}, \\ G_F &= G_{11} + G_{22}. \end{aligned} \quad (4)$$

The inverted relations read

$$\begin{aligned} G_{11} &= \frac{1}{2} (G_F + G_A + G_R), \\ G_{12} &= \frac{1}{2} (G_F + G_A - G_R), \\ G_{21} &= \frac{1}{2} (G_F - G_A + G_R), \\ G_{22} &= \frac{1}{2} (G_F - G_A - G_R). \end{aligned} \quad (5)$$

The relations (3–5) also hold for full propagators.

Using (1) and (2) in (4), the free propagators are given in the Keldysh representation by

$$\begin{aligned} D_R(K) &= \frac{1}{K^2 - m^2 + i \operatorname{sgn}(k_0)\epsilon}, \\ D_A(K) &= \frac{1}{K^2 - m^2 - i \operatorname{sgn}(k_0)\epsilon}, \\ D_F(K) &= (1 + 2n_B(k_0)) \operatorname{sgn}(k_0) (D_R(K) - D_A(K)) = -2\pi i (1 + 2n_B(k_0)) \delta(K^2 - m^2) \end{aligned} \quad (6)$$

for bosons and

$$\begin{aligned} S_R(K) &= \frac{\not{K} + m}{K^2 - m^2 + i \operatorname{sgn}(k_0)\epsilon} = (\not{K} + m) \bar{D}_R(K), \\ S_A(K) &= \frac{\not{K} + m}{K^2 - m^2 - i \operatorname{sgn}(k_0)\epsilon} = (\not{K} + m) \bar{D}_A(K), \\ S_F(K) &= (1 - 2n_F(k_0)) \operatorname{sgn}(k_0) (S_R(K) - S_A(K)) \\ &= -2\pi i (\not{K} + m) (1 - 2n_F(k_0)) \delta(K^2 - m^2) = (\not{K} + m) \bar{D}_F(K) \end{aligned} \quad (7)$$

for fermions, where the last equation in each of (6) and (7) is a consequence of the dissipation-fluctuation theorem. Although  $\bar{D}_{A,R} = D_{A,R}$  we keep the bar in our notation to more easily recognize fermion and boson propagators in the calculations below.

### III. SPECTRAL REPRESENTATION OF THE 4-POINT VERTEX

In this section we briefly review some useful relations among the different thermal components of the 4-point functions, and we derive their spectral representations. Some of these relations have already been reported in the literature [14–16,24] using different notation. We discuss these results at the end of this section. For any 1PI four-point function we define the four incoming external momenta as  $P_1, P_2, P_3$ , and  $P_4 = -(P_1 + P_2 + P_3)$ . In this section we suppress all indices except Keldysh indices.

#### A. Largest and smallest time equations

If  $t_4$  is the largest time argument, one can obtain the “largest time equations” [14,15,24]:

$$\theta_{43} \theta_{32} \theta_{21} (G_{abc1} + G_{abc2}) = \theta_{43} \theta_{31} \theta_{12} (G_{abc1} + G_{abc2}) = 0, \quad (8a)$$

$$\theta_{42} \theta_{23} \theta_{31} (G_{abc1} + G_{abc2}) = \theta_{42} \theta_{23} \theta_{13} (G_{abc1} + G_{abc2}) = 0, \quad (8b)$$

$$\theta_{41} \theta_{13} \theta_{32} (G_{abc1} + G_{abc2}) = \theta_{41} \theta_{12} \theta_{23} (G_{abc1} + G_{abc2}) = 0, \quad (8c)$$

$$\theta_{32} \theta_{21} \theta_{14} (G_{ab1c} + G_{ab2c}) = \theta_{31} \theta_{12} \theta_{24} (G_{ab1c} + G_{ab2c}) = 0, \quad (8d)$$

$$\theta_{23} \theta_{34} \theta_{41} (G_{a1bc} + G_{a2bc}) = \theta_{24} \theta_{43} \theta_{31} (G_{a1bc} + G_{a2bc}) = 0, \quad (8e)$$

$$\theta_{13} \theta_{32} \theta_{24} (G_{1abc} + G_{2abc}) = \theta_{12} \theta_{23} \theta_{34} (G_{1abc} + G_{2abc}) = 0, \quad (8f)$$

where  $a, b, c$  can be either 1 or 2, and  $\theta_{ij} \equiv \theta(t_i - t_j)$  is the step function.

By tilde conjugation (which replaces time ordering with anti-time ordering [21,23]) one obtains equations of the form:

$$\theta_{12} \theta_{23} \theta_{34} (\tilde{G}_{abc1} + \tilde{G}_{abc2}) = \theta_{13} \theta_{32} \theta_{24} (\tilde{G}_{abc1} + \tilde{G}_{abc2}) = 0, \quad (9a)$$

$$\theta_{41} \theta_{12} \theta_{23} (\tilde{G}_{ab1c} + \tilde{G}_{ab2c}) = \theta_{42} \theta_{21} \theta_{13} (\tilde{G}_{ab1c} + \tilde{G}_{ab2c}) = 0, \quad (9b)$$

$$\theta_{14} \theta_{43} \theta_{32} (\tilde{G}_{a1bc} + \tilde{G}_{a2bc}) = \theta_{13} \theta_{34} \theta_{42} (\tilde{G}_{a1bc} + \tilde{G}_{a2bc}) = 0, \quad (9c)$$

$$\theta_{42} \theta_{23} \theta_{31} (\tilde{G}_{1abc} + \tilde{G}_{2abc}) = \theta_{43} \theta_{32} \theta_{21} (\tilde{G}_{1abc} + \tilde{G}_{2abc}) = 0, \quad (9d)$$

Eqs. (8) and (9) are the analogues of the “largest time equations” and “smallest time equations”, respectively, of Ref. [14]. They will be used extensively in the derivation of the spectral representations below. Their generalization to arbitrary  $n$ -point functions is straightforward.

#### B. Derivation of spectral representations

One can construct the “retarded–advanced” vertex functions from the sixteen components of the real-time 4-point function as in [19,21]. The KMS conditions allows to reduce them to the following seven combinations [25,26]:

$$G_{raaa} = G_{1111} + G_{1211} + G_{1121} + G_{1112} + G_{1122} + G_{1221} + G_{1212} + G_{1222}, \quad (10a)$$

$$G_{araa} = G_{1111} + G_{2111} + G_{1121} + G_{1112} + G_{1122} + G_{2121} + G_{2112} + G_{2122}, \quad (10b)$$

$$G_{aara} = G_{1111} + G_{2111} + G_{1211} + G_{1112} + G_{1212} + G_{2211} + G_{2112} + G_{2212}, \quad (10c)$$

$$G_{aaar} = G_{1111} + G_{2111} + G_{1211} + G_{1121} + G_{1221} + G_{2211} + G_{2121} + G_{2221}, \quad (10d)$$

$$G_{rara} = G_{1111} + G_{1211} + G_{1112} + G_{1212} + G_{2121} + G_{2122} + G_{2221} + G_{2222}, \quad (10e)$$

$$G_{rraa} = G_{1111} + G_{1112} + G_{1121} + G_{1122} + G_{2211} + G_{2212} + G_{2221} + G_{2222}, \quad (10f)$$

$$G_{raar} = G_{1111} + G_{1121} + G_{1211} + G_{1221} + G_{2112} + G_{2122} + G_{2212} + G_{2222}. \quad (10g)$$

It is straightforward to show that the first four are the standard retarded vertex functions

$$G_{raaa} = G_{R1}; \quad G_{araa} = G_{R2}; \quad G_{aara} = G_{R3}; \quad G_{aaar} = G_{R4}. \quad (11)$$

The last three we will call “mixed retarded-advanced” functions.

There are eight other vertices which one can obtain from (10) using the KMS conditions [25,26]. We write down only the three which we need:

$$G_{arar} = G_{1111} + G_{1121} + G_{2111} + G_{2121} + G_{1212} + G_{1222} + G_{2212} + G_{2222}, \quad (12a)$$

$$G_{arra} = G_{1111} + G_{1112} + G_{2111} + G_{2112} + G_{1221} + G_{1222} + G_{2221} + G_{2222}, \quad (12b)$$

$$G_{aarr} = G_{1111} + G_{1211} + G_{2111} + G_{2211} + G_{1122} + G_{1222} + G_{2122} + G_{2222}. \quad (12c)$$

We can re-express these vertices in terms of spectral functions by making use of various properties of theta functions. We will use

$$\theta_{12} + \theta_{21} = 1, \quad \theta_{12}\theta_{21} = 0, \quad \theta_{23}\theta_{34}\theta_{24} = \theta_{23}\theta_{34}. \quad (13)$$

(i) We begin with  $G_{R1}$ . We rewrite  $G_{R1}$  as

$$G_{R1} = (\theta_{23} + \theta_{32})(\theta_{34} + \theta_{43})(\theta_{24} + \theta_{42})G_{R1}. \quad (14)$$

Inserting the identities

$$\theta_{13}G_{R1} = \theta_{12}G_{R1} = \theta_{14}G_{R1} = G_{R1} \quad (15)$$

into (14) we obtain

$$\begin{aligned} G_{R1} = & \theta_{12}\theta_{23}\theta_{34}G_{R1} + \theta_{12}\theta_{24}\theta_{43}G_{R1} + \theta_{14}\theta_{42}\theta_{23}G_{R1} \\ & + \theta_{14}\theta_{43}\theta_{32}G_{R1} + \theta_{13}\theta_{34}\theta_{42}G_{R1} + \theta_{13}\theta_{32}\theta_{24}G_{R1}. \end{aligned} \quad (16)$$

Using the identities

$$\begin{aligned} \theta(1ijk)G_{R2} &= \theta_{1i}\theta_{ij}\theta_{jk}G_{R2} = 0, \\ \theta(1ijk)G_{R3} &= \theta_{1i}\theta_{ij}\theta_{jk}G_{R3} = 0, \\ \theta(1ijk)G_{R4} &= \theta_{1i}\theta_{ij}\theta_{jk}G_{R4} = 0, \quad (i, j, k = 2, 3, 4) \end{aligned} \quad (17)$$

which result from conflicting  $\theta$ -functions, we have

$$\begin{aligned} G_{R1} &= [\theta(1234) + \theta(1243) + \theta(1324) + \theta(1342) + \theta(1423) + \theta(1432)] (G_{R1} - G_{R2} + G_{R3} - G_{R4}) \\ &= [\theta(1234) + \theta(1243) + \theta(1324) + \theta(1342) + \theta(1423) + \theta(1432)] \rho_{12} \end{aligned} \quad (18)$$

with

$$\begin{aligned} \rho_{12} &= G_{R1} - G_{R2} + G_{R3} - G_{R4} \\ &= G_{1211} - G_{2122} + 2(G_{1212} - G_{2121}) + G_{1112} - G_{2221} + G_{1222} - G_{2111} + G_{2212} - G_{1121}. \end{aligned} \quad (19)$$

(ii) For  $G_{R2}$ ,  $G_{R3}$  and  $G_{R4}$  one proceeds similarly and obtains

$$G_{R2} = [\theta(2134) + \theta(2143) + \theta(2314) + \theta(2341) + \theta(2413) + \theta(2431)](-\rho_{12}), \quad (20a)$$

$$G_{R3} = [\theta(3124) + \theta(3142) + \theta(3214) + \theta(3241) + \theta(3412) + \theta(3421)] \rho_{12}, \quad (20b)$$

$$G_{R4} = [\theta(4123) + \theta(4132) + \theta(4213) + \theta(4231) + \theta(4312) + \theta(4321)](-\rho_{12}). \quad (20c)$$

(iii) The procedure for the mixed retarded-advanced four-point functions is similar. We write

$$G_{rraa} = (\theta_{12} + \theta_{21})(\theta_{14} + \theta_{41})(\theta_{23} + \theta_{32})(\theta_{34} + \theta_{43})(\theta_{24} + \theta_{42})G_{rraa} \quad (21)$$

and use

$$\begin{aligned} \theta(3ijk)G_{rraa} &= 0, \quad i, j, k = 1, 2, 4, \\ \theta(4ijk)G_{rraa} &= 0, \quad i, j, k = 1, 3, 4, \end{aligned} \quad (22)$$

to obtain

$$G_{rraa} = [\theta(1234) + \theta(1243) + \theta(1324) + \theta(1342) + \theta(1423) + \theta(1432) + \theta(2134) + \theta(2143) + \theta(2314) + \theta(2341) + \theta(2413) + \theta(2431)] G_{rraa}. \quad (23)$$

Using the identities

$$\begin{aligned} \theta(1ijk)\tilde{G}_{rraa} &= 0, \quad i, j, k = 2, 3, 4, \\ \theta(2ijk)\tilde{G}_{rraa} &= 0, \quad i, j, k = 1, 3, 4 \end{aligned} \quad (24)$$

allows us to write

$$G_{rraa} = [\theta(1234) + \theta(1243) + \theta(1324) + \theta(1342) + \theta(1423) + \theta(1432) + \theta(2134) + \theta(2143) + \theta(2314) + \theta(2341) + \theta(2413) + \theta(2431)] \rho_3 \quad (25)$$

with

$$\rho_3 = G_{rraa} - \tilde{G}_{rraa}. \quad (26)$$

Analogously, we can derive

$$G_{rara} = [\theta(1234) + \theta(1243) + \theta(1324) + \theta(1342) + \theta(1423) + \theta(1432) + \theta(3124) + \theta(3142) + \theta(3214) + \theta(3241) + \theta(3412) + \theta(3421)] \rho_4 \quad (27a)$$

$$G_{raar} = [\theta(1234) + \theta(1243) + \theta(1324) + \theta(1342) + \theta(1423) + \theta(1432) + \theta(4123) + \theta(4132) + \theta(4213) + \theta(4231) + \theta(4321) + \theta(4312)] \rho_5 \quad (27b)$$

where

$$\rho_4 = G_{rara} - \tilde{G}_{rara} \quad (28a)$$

$$\rho_5 = G_{raar} - \tilde{G}_{raar} \quad (28b)$$

Using the Fourier integral representation of the  $\theta$  function,

$$\theta_{ij} = -\frac{1}{2\pi i} \int_{-\infty}^{\infty} d\Omega \frac{e^{-i\Omega(t_i - t_j)}}{\Omega + i\epsilon}, \quad (29)$$

it is straightforward to derive the spectral integral representations in momentum space:

$$G_{R1}(\omega_1, \omega_2, \omega_3, \omega_4) = \oint a_1^+ [a_{12}^+(a_3^- + a_4^-) + a_{13}^+(a_2^- + a_4^-) + a_{14}^+(a_2^- + a_3^-)] \rho_{12}, \quad (30a)$$

$$G_{R2}(\omega_1, \omega_2, \omega_3, \omega_4) = \oint a_2^+ [a_{21}^+(a_3^- + a_4^-) + a_{23}^+(a_1^- + a_4^-) + a_{24}^+(a_1^- + a_3^-)] (-\rho_{12}), \quad (30b)$$

$$G_{R3}(\omega_1, \omega_2, \omega_3, \omega_4) = \oint a_3^+ [a_{31}^+(a_2^- + a_4^-) + a_{32}^+(a_1^- + a_4^-) + a_{34}^+(a_1^- + a_2^-)] \rho_{12}, \quad (30c)$$

$$G_{R4}(\omega_1, \omega_2, \omega_3, \omega_4) = \oint a_4^+ [a_{41}^+(a_2^- + a_3^-) + a_{42}^+(a_1^- + a_3^-) + a_{43}^+(a_1^- + a_2^-)] (-\rho_{12}), \quad (30d)$$

$$\begin{aligned} G_{rraa}(\omega_1, \omega_2, \omega_3, \omega_4) &= \oint \left( a_1^+ [a_{12}^+(a_3^- + a_4^-) + a_{13}^+(a_2^- + a_4^-) + a_{14}^+(a_2^- + a_3^-)] \right. \\ &\quad \left. + a_2^+ [a_{21}^+(a_3^- + a_4^-) + a_{23}^+(a_1^- + a_4^-) + a_{24}^+(a_1^- + a_3^-)] \right) \rho_3, \end{aligned} \quad (30e)$$

$$\begin{aligned} G_{rara}(\omega_1, \omega_2, \omega_3, \omega_4) &= \oint \left( a_1^+ [a_{12}^+(a_3^- + a_4^-) + a_{13}^+(a_2^- + a_4^-) + a_{14}^+(a_2^- + a_3^-)] \right. \\ &\quad \left. + a_3^+ [a_{31}^+(a_2^- + a_4^-) + a_{32}^+(a_1^- + a_4^-) + a_{34}^+(a_1^- + a_2^-)] \right) \rho_4 \end{aligned} \quad (30f)$$

$$\begin{aligned} G_{raar}(\omega_1, \omega_2, \omega_3, \omega_4) &= \oint \left( a_1^+ [a_{12}^+(a_3^- + a_4^-) + a_{13}^+(a_2^- + a_4^-) + a_{14}^+(a_2^- + a_3^-)] \right. \\ &\quad \left. + a_4^+ [a_{41}^+(a_2^- + a_3^-) + a_{42}^+(a_1^- + a_3^-) + a_{43}^+(a_1^- + a_2^-)] \right) \rho_5 \end{aligned} \quad (30g)$$

where

$$\oint = \frac{i}{(2\pi)^3} \int d\Omega_1 d\Omega_2 d\Omega_3 \quad (31a)$$

$$a_i^\pm = \frac{1}{\omega_i - \Omega_i \pm i\epsilon} \quad (31b)$$

$$a_{ij}^\pm = \frac{1}{\omega_i + \omega_j - \Omega_j - \Omega_j \pm i\epsilon}; \quad i, j = 1, 2, 3, 4. \quad (31c)$$

The frequency arguments of the spectral functions under the integrals are  $\rho_i(\Omega_1, \Omega_2, \Omega_3, \Omega_4)$  with  $\Omega_1 + \Omega_2 + \Omega_3 + \Omega_4 = 0$ . The spatial momenta  $\mathbf{p}_1, \mathbf{p}_2, \mathbf{p}_3$ , and  $\mathbf{p}_4 = -(\mathbf{p}_1 + \mathbf{p}_2 + \mathbf{p}_3)$  are the same on both sides of these equations and have therefore been suppressed.

We have written the seven vertex functions (10) in terms of one complex spectral density ( $\rho_{12} \equiv \rho_1 + i\rho_2$ ) and three purely imaginary spectral densities ( $\rho_3, \rho_4, \rho_5$ ). This means that all sixteen 4-point functions can be expressed in terms of five real spectral densities:

$$\rho_1 = \text{Re} [n_B^{-1}(p_{20})G_{2122} + 2n_B^{-1}(p_{20} + p_{40})G_{2121} + n_B^{-1}(p_{40})G_{2221} - n_B^{-1}(p_{10})G_{1222} - n_B^{-1}(p_{30})G_{2212}], \quad (32a)$$

$$\rho_2 = -\text{Im} [n_F^{-1}(p_{20})G_{2122} + 2n_F^{-1}(p_{20} + p_{40})G_{2121} + n_F^{-1}(p_{40})G_{2221} - n_F^{-1}(p_{10})G_{1222} - n_F^{-1}(p_{30})G_{2212}], \quad (32b)$$

$$\bar{\rho}_3 = -i\rho_3 = 2 \text{Im} G_{rraa}, \quad (32c)$$

$$\bar{\rho}_4 = -i\rho_4 = 2 \text{Im} G_{rara}, \quad (32d)$$

$$\bar{\rho}_5 = -i\rho_5 = 2 \text{Im} G_{raar}, \quad (32e)$$

where we used the following relations in momentum space resulting from the KMS condition [21]:

$$G_{1211} = e^{\beta p_{20}} G_{2122}^*, \quad G_{1212} = e^{\beta(p_{20} + p_{40})} G_{2121}^*, \quad G_{1112} = e^{\beta p_{40}} G_{2221}^*, \quad (33a)$$

$$G_{2111} = e^{\beta p_{10}} G_{1222}^*, \quad G_{1121} = e^{\beta p_{30}} G_{2212}^*, \quad (33b)$$

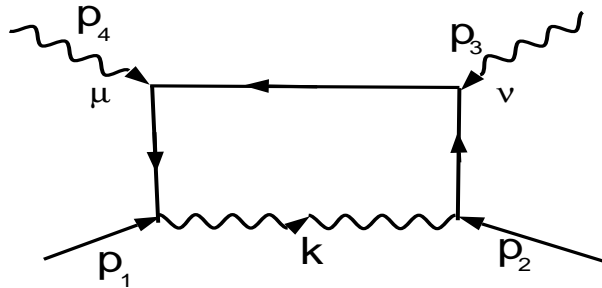
$$\tilde{G}_{rraa} = G_{rraa}^*, \quad \tilde{G}_{rara} = G_{rara}^*, \quad \tilde{G}_{raar} = G_{raar}^*. \quad (33c)$$

These results should be compared with the expressions derived in [15] in which the spectral representations for the four retarded functions  $G_{Ri}$ ,  $i = 1, 2, 3, 4$  were given in terms of three real spectral densities. A relation between these three spectral densities exists which can be employed to reduce the number of independent spectral functions to two; this is consistent with our result. Spectral representations for the mixed retarded-advanced 4-point functions have also been previously discussed: in [17], using a different definition of the mixed retarded-advanced 4-point functions, the spectral representation for one of these vertices was given in terms of six spectral densities.

We finally note that in deriving the spectral representations (30) no use was made of the KMS condition. In this form, (with the spectral densities defined by (16), (26) and (28)), Eqs. (30) remain valid out of thermal equilibrium.

#### IV. 4-POINT VERTEX FUNCTIONS IN QED IN THE HTL APPROXIMATION

In this section, we calculate the seven 4-point vertex functions (10) for QED in the HTL approximation. In the HTL approximation QED has two non-zero 4-point vertex functions, shown in Fig. [1] below:



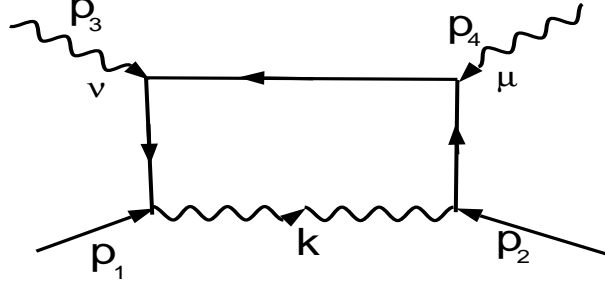


Fig. [1]: 4-point vertex in QED (a - upper graph) and its cross term (b - lower graph).

The other two 4-point vertex functions (four-photon vertex and four-fermion vertex) are zero in the HTL approximation [3]. We calculate the diagrams in Fig. [1] as follows: the real-time Green functions are written in the Keldysh formalism using (5) and (10). The photon propagator in the Feynman gauge is given by  $-ig_{\mu\nu}D(K)$  where  $D(K)$  is defined in (6). The fermion propagator is defined in (7). For the diagram in Fig. [1a] we obtain

$$G_{R1}^{\mu\nu(a)}(P_1, P_2, P_3, P_4) = \frac{1}{2} \int \frac{d^4 K}{(2\pi)^4} H^{\mu\nu}(K) [a_1 \bar{a}_2 \bar{a}_3 \bar{a}_4 + r_1 \bar{r}_2 \bar{r}_3 \bar{r}_4 + f_1 \bar{a}_2 \bar{a}_3 \bar{a}_4 + r_1 \bar{f}_2 \bar{a}_3 \bar{a}_4 + r_1 \bar{r}_2 \bar{f}_3 \bar{a}_4 + r_1 \bar{r}_2 \bar{r}_3 \bar{f}_4], \quad (34a)$$

$$G_{R2}^{\mu\nu(a)}(P_1, P_2, P_3, P_4) = \frac{1}{2} \int \frac{d^4 K}{(2\pi)^4} H^{\mu\nu}(K) [a_1 \bar{a}_2 \bar{a}_3 \bar{a}_4 + r_1 \bar{r}_2 \bar{r}_3 \bar{r}_4 + f_1 \bar{r}_2 \bar{r}_3 \bar{r}_4 + a_1 \bar{f}_2 \bar{a}_3 \bar{a}_4 + a_1 r_2 \bar{f}_3 \bar{a}_4 + a_1 \bar{r}_2 r_3 \bar{f}_4], \quad (34b)$$

$$G_{R3}^{\mu\nu(a)}(P_1, P_2, P_3, P_4) = \frac{1}{2} \int \frac{d^4 K}{(2\pi)^4} H^{\mu\nu}(K) [a_1 \bar{a}_2 \bar{a}_3 \bar{a}_4 + r_1 \bar{r}_2 \bar{r}_3 \bar{r}_4 + f_1 \bar{a}_2 \bar{r}_3 \bar{r}_4 + r_1 \bar{f}_2 \bar{r}_3 \bar{r}_4 + a_1 \bar{a}_2 \bar{f}_3 \bar{a}_4 + a_1 \bar{a}_2 \bar{r}_3 \bar{f}_4], \quad (34c)$$

$$G_{R4}^{\mu\nu(a)}(P_1, P_2, P_3, P_4) = \frac{1}{2} \int \frac{d^4 K}{(2\pi)^4} H^{\mu\nu}(K) [a_1 \bar{a}_2 \bar{a}_3 \bar{a}_4 + r_1 \bar{r}_2 \bar{r}_3 \bar{r}_4 + f_1 \bar{a}_2 \bar{a}_3 \bar{r}_4 + r_1 \bar{f}_2 \bar{a}_3 \bar{r}_4 + r_1 \bar{r}_2 \bar{f}_3 \bar{r}_4 + a_1 \bar{a}_2 \bar{a}_3 \bar{f}_4], \quad (34d)$$

$$G_{raaa}^{\mu\nu(a)}(P_1, P_2, P_3, P_4) = \frac{1}{2} \int \frac{d^4 K}{(2\pi)^4} H^{\mu\nu}(K) [a_1 \bar{a}_2 \bar{a}_3 \bar{a}_4 + r_1 \bar{r}_2 \bar{r}_3 \bar{r}_4 + f_1 \bar{a}_2 \bar{f}_3 \bar{a}_4 + r_1 \bar{a}_4 \bar{f}_2 \bar{f}_3 + r_1 \bar{r}_2 \bar{a}_3 \bar{a}_4 + f_1 \bar{a}_2 \bar{r}_3 \bar{f}_4 + r_1 \bar{r}_3 \bar{f}_2 \bar{f}_4 + a_1 \bar{a}_2 \bar{r}_3 \bar{r}_4], \quad (34e)$$

$$G_{rraa}^{\mu\nu(a)}(P_1, P_2, P_3, P_4) = \frac{1}{2} \int \frac{d^4 K}{(2\pi)^4} H^{\mu\nu}(K) [a_1 \bar{a}_2 \bar{a}_3 \bar{a}_4 + r_1 \bar{r}_2 \bar{r}_3 \bar{r}_4 + r_1 \bar{a}_2 \bar{a}_3 \bar{a}_4 + a_1 \bar{r}_2 \bar{r}_3 \bar{r}_4 + f_1 \bar{f}_2 \bar{a}_3 \bar{a}_4 + f_1 \bar{f}_3 \bar{r}_2 \bar{a}_4 + f_1 \bar{f}_4 \bar{r}_2 \bar{r}_3], \quad (34f)$$

$$G_{raar}^{\mu\nu(a)}(P_1, P_2, P_3, P_4) = \frac{1}{2} \int \frac{d^4 K}{(2\pi)^4} H^{\mu\nu}(K) [a_1 \bar{a}_2 \bar{a}_3 \bar{a}_4 + r_1 \bar{r}_2 \bar{r}_3 \bar{r}_4 + a_1 \bar{a}_2 \bar{a}_3 \bar{r}_4 + r_1 \bar{r}_2 \bar{r}_3 \bar{a}_4 + f_1 \bar{f}_4 \bar{a}_2 \bar{a}_3 + \bar{f}_2 \bar{f}_4 r_1 \bar{a}_3 + \bar{f}_3 \bar{f}_4 r_1 \bar{r}_2], \quad (34g)$$

where

$$H_{\mu\nu}(K) = e^4 \gamma_\alpha (\not{K} - \not{P}_1 + m) \gamma_\mu (\not{P}_2 + \not{P}_3 + \not{K} + m) \gamma_\nu (\not{P}_2 + \not{K} + m) \gamma_\alpha \quad (35)$$

and we used the notation  $a_1 = D_A(K)$ ,  $r_1 = D_R(K)$ ,  $f_1 = D_F(K)$  for photon propagators and  $\bar{a}_j = \bar{D}_A(K_j)$ ,  $\bar{r}_j = \bar{D}_R(K_j)$ ,  $\bar{f}_j = \bar{D}_F(K_j)$  [ $j = 2, 3, 4$  and  $K_2 = P_2 + K$ ,  $K_3 = P_2 + P_3 + K$ ,  $K_4 = K - P_1$ ] for electron propagators. Note that the first two terms in each equation of (34) vanish by contour integration since all poles are located on the same side of the real axis.

Before doing any momentum integrations, we can see immediately from (34) that the one-loop retarded functions ( $G_{Ri}$ ,  $i = 1, 2, 3, 4$ ) are linear in the distribution functions, since they are linear in the symmetric propagators  $f_i$  and/or  $\bar{f}_i$ . Terms with higher powers of the distribution functions are explicitly cancelled in the Keldysh formalism. This type of cancellation also occurs for the 2- and 3-point retarded-advanced functions [27]. In contrast, the mixed

retarded-advanced functions are bilinear in the distribution functions. One of the advantages of the Keldysh formalism is that it allows us to immediately identify the leading order temperature dependence.

In the HTL approximation, the external momenta are soft (of order  $eT$  with  $e \ll 1$ ) and the loop momenta are hard (of order  $T$ ) [4,5]. In this approximation, we can neglect the external momenta and the bare electron mass  $m$  relative to the loop momenta. For  $H_{\mu\nu}(K)$  one then obtains

$$H_{\mu\nu}(K) \approx 8e^4 K_\mu K_\nu \bar{K}. \quad (36)$$

We first consider  $G_{R1}^a$ . Fig. [1a] gives

$$\begin{aligned} G_{R1}^{\mu\nu(a)}(P_1, P_2, P_3, P_4) &= \frac{1}{2} \int \frac{d^4 K}{(2\pi)^4} H^{\mu\nu}(K) [f_1 \bar{a}_2 \bar{a}_3 \bar{a}_4 + r_1 \bar{f}_2 \bar{a}_3 \bar{a}_4 + r_1 \bar{r}_2 \bar{f}_3 \bar{a}_4 + r_1 \bar{r}_2 \bar{r}_3 \bar{f}_4] \\ &= I_1 + I_2 + I_3 + I_4. \end{aligned} \quad (37)$$

From (6), (7) we have

$$\begin{aligned} a_i(K) &= \bar{a}_i(K) = \frac{1}{K^2 - m_i^2 - i \text{sgn}(k_0) \epsilon}, \\ r_i(K) &= \bar{r}_i(K) = \frac{1}{K^2 - m_i^2 + i \text{sgn}(k_0) \epsilon}, \\ f_1(K) &= -2\pi i \delta(K^2) (1 + 2n_B(k)), \\ \bar{f}_i(K) &= -2\pi i \delta(K^2 - m_i^2) (1 - 2n_F(k)), \end{aligned} \quad (38)$$

where  $i=2, 3, 4$  and  $m_2=m_3=m_4=m$  which stands for the electron mass. We calculate the contribution from each of the terms in (37) in the HTL approximation:  $K \sim T \gg P_1, P_2, P_3, P_4, m$ . For the temperature-dependent contributions we obtain

$$I_1 = \frac{ie^4}{(2\pi)^3} \int dk k n_B(k) \int d\Omega V^\mu V^\nu \bar{\Psi} \cdot b_{23}^- b_1^+ b_2^-, \quad (39a)$$

$$I_2 = \frac{ie^4}{(2\pi)^3} \int dk k n_F(k) \int d\Omega V^\mu V^\nu \bar{\Psi} \cdot b_2^- b_3^- b_{12}^+, \quad (39b)$$

$$I_3 = \frac{ie^4}{(2\pi)^3} \int dk k n_F(k) \int d\Omega V^\mu V^\nu \bar{\Psi} \cdot b_3^- b_4^- b_{23}^-, \quad (39c)$$

$$I_4 = -\frac{ie^4}{(2\pi)^3} \int dk k n_F(k) \int d\Omega V^\mu V^\nu \bar{\Psi} \cdot b_1^+ b_4^- b_{12}^+, \quad (39d)$$

where

$$b_i^\pm = \frac{1}{P_i \cdot V \pm i\epsilon}, \quad (40a)$$

$$b_{ij}^\pm = \frac{1}{(P_i + P_j) \cdot V \pm i\epsilon}, \quad i, j = 1, 2, 3, 4, \quad (40b)$$

and  $V = (1, \mathbf{V})$  with  $\mathbf{V} = \mathbf{k}/k$  a light-like unit vector, and  $\int d\Omega$  denotes integration over the orientation of  $\mathbf{V}$ .

By interchanging  $P_3$  and  $P_4$  we obtain the contribution from Fig. [1b] to  $G_{R1}$ :

$$G_{R1}^{\mu\nu(b)} = J_1 + J_2 + J_3 + J_4, \quad (41)$$

with

$$J_1 = \frac{ie^4}{(2\pi)^3} \int dk k n_B(k) \int d\Omega V^\mu V^\nu \bar{\Psi} \cdot b_1^+ b_2^- b_{24}^-, \quad (42a)$$

$$J_2 = \frac{ie^4}{(2\pi)^3} \int dk k n_F(k) \int d\Omega V^\mu V^\nu \bar{\Psi} \cdot b_2^- b_4^- b_{12}^+, \quad (42b)$$

$$J_3 = \frac{ie^4}{(2\pi)^3} \int dk k n_F(k) \int d\Omega V^\mu V^\nu \bar{\Psi} \cdot b_3^- b_4^- b_{24}^-, \quad (42c)$$

$$J_4 = -\frac{ie^4}{(2\pi)^3} \int dk k n_F(k) \int d\Omega V^\mu V^\nu \bar{\Psi} \cdot b_1^+ b_4^- b_{12}^+. \quad (42d)$$

Combining (39) and (42), the total contribution to  $G_{R1}^{\mu\nu}$  from Fig. [1] reads

$$G_{R1}^{\mu\nu}(P_1, P_2, P_3, P_4) = G_{R1}^{\mu\nu(a)} + G_{R1}^{\mu\nu(b)} = \frac{ie^2 m_\beta^2}{4\pi} \int d\Omega V^\mu V^\nu \mathcal{V} \cdot b_{23}^- b_{24}^- (b_1^+ - b_2^-) \quad (43)$$

where

$$m_\beta^2 = \frac{e^2}{2\pi^2} \int dk k (n_B(k) + n_F(k)) = \frac{e^2 T^2}{8} \quad (44)$$

is the usual expression for the square of the dynamically generated thermal electron mass.

Proceeding similarly, we can calculate the other three retarded 4-point functions in finite temperature QED in the HTL approximation. The final results, including both diagrams in Fig. [1], are

$$G_{R2}^{\mu\nu}(P_1, P_2, P_3, P_4) = \frac{ie^2 m_\beta^2}{4\pi} \int d\Omega V^\mu V^\nu \mathcal{V} b_{23}^+ b_{24}^+ (b_1^- - b_2^+), \quad (45a)$$

$$G_{R3}^{\mu\nu}(P_1, P_2, P_3, P_4) = \frac{ie^2 m_\beta^2}{4\pi} \int d\Omega V^\mu V^\nu \mathcal{V} b_{23}^+ b_{24}^+ (b_1^- - b_2^-), \quad (45b)$$

$$G_{R4}^{\mu\nu}(P_1, P_2, P_3, P_4) = \frac{ie^2 m_\beta^2}{4\pi} \int d\Omega V^\mu V^\nu \mathcal{V} b_{23}^- b_{24}^- (b_1^- - b_2^-). \quad (45c)$$

Our results agree with those obtained in the ITF [18]; to leading order, all of the retarded 4-point functions are proportional to  $T^2$ .

Next we consider the mixed retarded-advanced 4-point functions. We begin with  $G_{rara}^{\mu\nu}$ . The leading order temperature-dependent piece from Fig. [1a] is

$$\begin{aligned} G_{rara}^{\mu\nu(a)}(P_1, P_2, P_3, P_4) &= \frac{1}{2} \int \frac{d^4 K}{(2\pi)^4} H^{\mu\nu}(K) [f_1 \bar{a}_2 \bar{f}_3 \bar{a}_4 + r_1 \bar{f}_2 \bar{f}_3 \bar{a}_4 + f_1 \bar{a}_2 \bar{r}_3 \bar{f}_4 + r_1 \bar{r}_3 \bar{f}_2 \bar{f}_4] \\ &= T_1 + T_2 + T_3 + T_4, \end{aligned} \quad (46)$$

where the functions  $T_i$ ;  $i = \{1, 2, 3, 4\}$  represent the contributions of the four terms respectively. Inserting the propagators (38) and using the HTL approximation we find

$$T_1 = \frac{e^4}{(2\pi)^3} c_\beta \int d\Omega V^\mu V^\nu \mathcal{V} b_1^+ b_2^- (b_{23}^- - b_{23}^+), \quad (47a)$$

$$T_2 = \frac{e^4}{(2\pi)^3} d_\beta \int d\Omega V^\mu V^\nu \mathcal{V} b_{12}^+ b_2^- (b_3^- - b_3^+), \quad (47b)$$

$$T_3 = \frac{e^4}{(2\pi)^3} c_\beta \int d\Omega V^\mu V^\nu \mathcal{V} b_2^- b_{23}^+ (b_1^+ - b_1^-), \quad (47c)$$

$$T_4 = \frac{e^4}{(2\pi)^3} d_\beta \int d\Omega V^\mu V^\nu \mathcal{V} b_3^+ b_2^- (b_{12}^+ - b_{12}^-), \quad (47d)$$

where

$$\begin{aligned} c_\beta &= \int dk k [n_B(k)(1-n_F(k)) - n_F(k)(1+n_B(k))], \\ d_\beta &= -2 \int dk k n_F(k)(1-n_F(k)). \end{aligned} \quad (48)$$

Inserting the standard forms for the Bose-Einstein and Fermi-Dirac distributions we obtain in thermal equilibrium

$$c_\beta = 0, \quad d_\beta = -(2 \ln 2) T^2. \quad (49)$$

The contribution from Fig. [1b] to  $G_{rara}^{\mu\nu}$  is

$$G_{rara}^{\mu\nu(b)} = S_1 + S_2 + S_3 + S_4 \quad (50)$$

with

$$S_1 = \frac{e^4}{(2\pi)^3} c_\beta \int d\Omega V^\mu V^\nu \mathcal{V} b_1^+ b_2^- (b_{24}^- - b_{24}^+), \quad (51a)$$

$$S_2 = \frac{e^4}{(2\pi)^3} d_\beta \int d\Omega V^\mu V^\nu \mathcal{V} b_{12}^+ b_2^- (b_4^- - b_4^+), \quad (51b)$$

$$S_3 = \frac{e^4}{(2\pi)^3} c_\beta \int d\Omega V^\mu V^\nu \mathcal{V} b_2^- b_{24}^+ (b_1^+ - b_1^-), \quad (51c)$$

$$S_4 = \frac{e^4}{(2\pi)^3} d_\beta \int d\Omega V^\mu V^\nu \mathcal{V} b_4^+ b_2^- (b_{12}^+ - b_{12}^-). \quad (51d)$$

Adding (47) and (51) we obtain

$$G_{rara}^{\mu\nu} = \frac{e^4}{(2\pi)^3} \int d\Omega V^\mu V^\nu \mathcal{V} \left[ d_\beta b_2^- (b_{12}^+ (b_3^- + b_4^-) - b_{12}^- (b_3^+ + b_4^+)) + c_\beta b_2^- (b_1^+ (b_{23}^- + b_{24}^-) - b_1^- (b_{24}^+ + b_{23}^+)) \right]. \quad (52)$$

In spite of (49) we keep the terms  $\sim c_\beta$  because we will discuss the extension of these results to non-equilibrium situations in Sec. VII.

The other two mixed retarded-advanced 4-point functions are similarly calculated:

$$\begin{aligned} G_{raar}^{\mu\nu} &= \frac{e^4}{(2\pi)^3} \int d\Omega V^\mu V^\nu \mathcal{V} \left[ d_\beta b_1^+ (b_{12}^+ (b_3^- + b_4^-) - b_{12}^- (b_3^+ + b_4^+)) + c_\beta b_2^- (b_1^+ (b_{23}^- + b_{24}^-) - b_1^- (b_{24}^+ + b_{23}^+)) \right], \\ G_{rraa}^{\mu\nu} &= \frac{e^4}{(2\pi)^3} \int d\Omega V^\mu V^\nu \mathcal{V} \left[ c_\beta (b_2^- b_1^+ (b_{23}^- + b_{24}^-) - b_2^+ b_1^- (b_{24}^+ + b_{23}^+)) \right]. \end{aligned} \quad (53)$$

The last function vanishes in equilibrium since  $c_\beta = 0$ . The other mixed retarded-advanced 4-point functions are again proportional to  $T^2$ . Furthermore, since  $V^2=0$ , all seven 4-point functions are traceless ( $G_\mu^\mu = 0$ ) in the HTL approximation.

#### V. 4-POINT SPECTRAL FUNCTIONS IN HOT QED IN THE HTL APPROXIMATION

From (43), (45), (52) and (53) one obtains the following spectral representations for the 4-point retarded-advanced functions in the HTL approximation:

$$G_{R1}^{\mu\nu}(\omega_1, \omega_2, \omega_3, \omega_4) = \frac{i}{(2\pi)^3} \int d\Omega_1 d\Omega_2 d\Omega_3 d\Omega_4 \delta(\Omega_1 + \Omega_2 + \Omega_3 + \Omega_4) \rho_{\text{HTL}}^{\mu\nu}(\Omega_1, \Omega_2, \Omega_3, \Omega_4) a_{23}^- a_{24}^+ (a_1^+ - a_2^-), \quad (54a)$$

$$G_{R2}^{\mu\nu}(\omega_1, \omega_2, \omega_3, \omega_4) = \frac{i}{(2\pi)^3} \int d\Omega_1 d\Omega_2 d\Omega_3 d\Omega_4 \delta(\Omega_1 + \Omega_2 + \Omega_3 + \Omega_4) \rho_{\text{HTL}}^{\mu\nu}(\Omega_1, \Omega_2, \Omega_3, \Omega_4) a_{23}^+ a_{24}^+ (a_1^- - a_2^+), \quad (54b)$$

$$G_{R3}^{\mu\nu}(\omega_1, \omega_2, \omega_3, \omega_4) = \frac{i}{(2\pi)^3} \int d\Omega_1 d\Omega_2 d\Omega_3 d\Omega_4 \delta(\Omega_1 + \Omega_2 + \Omega_3 + \Omega_4) \rho_{\text{HTL}}^{\mu\nu}(\Omega_1, \Omega_2, \Omega_3, \Omega_4) a_{23}^+ a_{24}^+ (a_1^- - a_2^-), \quad (54c)$$

$$G_{R4}^{\mu\nu}(\omega_1, \omega_2, \omega_3, \omega_4) = \frac{i}{(2\pi)^3} \int d\Omega_1 d\Omega_2 d\Omega_3 d\Omega_4 \delta(\Omega_1 + \Omega_2 + \Omega_3 + \Omega_4) \rho_{\text{HTL}}^{\mu\nu}(\Omega_1, \Omega_2, \Omega_3, \Omega_4) a_{23}^- a_{24}^- (a_1^- - a_2^-), \quad (54d)$$

$$\begin{aligned} G_{rara}^{\mu\nu}(\omega_1, \omega_2, \omega_3, \omega_4) &= \frac{i}{(2\pi)^3} \int d\Omega_1 d\Omega_2 d\Omega_3 d\Omega_4 \delta(\Omega_1 + \Omega_2 + \Omega_3 + \Omega_4) \rho_{\text{HTL}}^{\mu\nu}(\Omega_1, \Omega_2, \Omega_3, \Omega_4) \\ &\quad \cdot \left[ \alpha_1 a_2^- (a_{12}^+ (a_3^- + a_4^-) - a_{12}^- (a_3^+ + a_4^+)) + \alpha_2 (a_2^- a_1^+ (a_{23}^- + a_{24}^-) - a_2^- a_1^- (a_{24}^+ + a_{23}^+)) \right], \end{aligned} \quad (54e)$$

$$\begin{aligned} G_{raar}^{\mu\nu}(\omega_1, \omega_2, \omega_3, \omega_4) &= \frac{i}{(2\pi)^3} \int d\Omega_1 d\Omega_2 d\Omega_3 d\Omega_4 \delta(\Omega_1 + \Omega_2 + \Omega_3 + \Omega_4) \rho_{\text{HTL}}^{\mu\nu}(\Omega_1, \Omega_2, \Omega_3, \Omega_4) \\ &\quad \cdot \left[ \alpha_1 a_1^+ (a_{12}^+ (a_3^- + a_4^-) - a_{12}^- (a_3^+ + a_4^+)) + \alpha_2 a_2^- a_1^+ (a_{23}^- + a_{24}^-) - a_2^- a_1^- (a_{24}^+ + a_{23}^+) \right], \end{aligned} \quad (54f)$$

$$\begin{aligned} G_{rraa}^{\mu\nu}(\omega_1, \omega_2, \omega_3, \omega_4) &= \frac{i}{(2\pi)^3} \int d\Omega_1 d\Omega_2 d\Omega_3 d\Omega_4 \delta(\Omega_1 + \Omega_2 + \Omega_3 + \Omega_4) \rho_{\text{HTL}}^{\mu\nu}(\Omega_1, \Omega_2, \Omega_3, \Omega_4) \\ &\quad \cdot \left[ \alpha_2 (a_2^- a_1^+ (a_{23}^- + a_{24}^-) - a_2^+ a_1^- (a_{24}^+ + a_{23}^+)) \right], \end{aligned} \quad (54g)$$

where

$$\rho_{\text{HTL}}^{\mu\nu}(\Omega_1, \Omega_2, \Omega_3, \Omega_4) = 2\pi^2 e^2 m_\beta^2 \int d\Omega V^\mu V^\nu \Psi \delta(\tilde{P}_1 \cdot V) \delta(\tilde{P}_2 \cdot V) \delta(\tilde{P}_3 \cdot V) \quad (55)$$

(with  $\tilde{P}_i^0 \equiv \Omega_i$ ,  $\tilde{\mathbf{P}}_i = \mathbf{P}_i$ ;  $i=\{1, 2, 3\}$  on the r.h.s.) and

$$\alpha_1 = \frac{d_\beta e^4}{2i\pi^2 e^2 m_\beta^2}; \quad \alpha_2 = \frac{c_\beta e^4}{2i\pi^2 e^2 m_\beta^2}. \quad (56)$$

These equations also hold in the non-equilibrium situations studied in Sec. VII. In equilibrium we use (49) to obtain

$$\alpha_1 = i \frac{8 \ln 2}{\pi^2}; \quad \alpha_2 = 0 \quad (57)$$

Note that the frequencies  $\Omega_i$  should not be confused with the angular factor  $\Omega$ . From  $V^2=0$  it follows that

$$(\rho_{\text{HTL}})^\mu_\mu = 0. \quad (58)$$

In contrast to the general spectral representations (30) of the 4-point functions given in Sec. III, in the HTL approximation the spectral representations (54) involve only a single, real-valued spectral density  $\rho_{\text{HTL}}^{\mu\nu}$ . This agrees with the result of Taylor [18] who showed for QCD in the ITF that in the HTL approximation all spectral densities degenerate to a single function. Clearly, the spectral density (55) is symmetric in the Lorentz indices and under interchange of the external momenta. Using the  $\delta$ -functions in (55) it is also easy to show that  $\rho_{\text{HTL}}^{\mu\nu}$  is transverse with respect to all external momenta:

$$P_\mu^i \rho_{\text{HTL}}^{\mu\nu} = 0, \quad i = 1, 2, 3, 4. \quad (59)$$

A previous RTF calculation of the 3-point spectral function in hot QED in the HTL approximation gave [26]

$$\rho_{\text{HTL}}^\mu(\Omega_1, \Omega_2, \Omega_3) = \frac{\pi e m_\beta^2}{2} \int d\Omega V^\mu \Psi \delta(\tilde{P}_1 \cdot V) \delta(\tilde{P}_2 \cdot V). \quad (60)$$

By comparing (55) with (59) we find the “sum rule”

$$\int d\Omega_3 \rho_{\text{HTL}}^{\mu 0}(\Omega_1, \Omega_2, \Omega_3, -(\Omega_1 + \Omega_2 + \Omega_3)) = 4\pi e \rho_{\text{HTL}}^\mu(\Omega_1, \Omega_2, -(\Omega_1 + \Omega_2)). \quad (61)$$

This agrees with the ITF results in [18]. A similar sum rule exists between the 2- and 3-point spectral densities: the 2-point spectral density is given by

$$\rho_{\text{HTL}}(\Omega_1, -\Omega_1) = \frac{m_\beta^2}{2} \int d\Omega \Psi \delta(\tilde{P}_1 \cdot V), \quad (62)$$

and the temporal component of the 3-point spectral density  $\rho_{\text{HTL}}^\mu(\Omega_1, \Omega_2, -(\Omega_1 + \Omega_2))$  obeys the sum rule

$$\int d\Omega_2 \rho_{\text{HTL}}^0(\Omega_1, \Omega_2, -(\Omega_1 + \Omega_2)) = \pi e \rho_{\text{HTL}}(\Omega_1, -\Omega_1). \quad (63)$$

We believe that analogous sum rules exist for the higher order  $n$ -point functions.

## VI. WARD IDENTITIES BETWEEN 3- AND 4-POINT FUNCTIONS IN THE HTL APPROXIMATION

In this section, we verify the HTL Ward identities between the 3- and 4-point vertex functions in QED, without doing momentum integrations. We split propagators in the integral expressions (34) by using the identities [28]

$$\bar{D}_{R/A}(K_2) \bar{D}_{R/A}(K_3) = \frac{1}{K_3^2 - K_2^2} (\bar{D}_{R/A}(K_2) - \bar{D}_{R/A}(K_3)) \quad (64)$$

This trick allows us to rewrite (34) as

$$G_{R1}^{\mu\nu(a)} = e^4 \int \frac{d^4 K}{(2\pi)^4} \frac{4K^\mu K^\nu K}{2P_3 \cdot K} [f_1(\bar{a}_2 - \bar{a}_3)\bar{a}_4 + r_1\bar{f}_2\bar{a}_4 - r_1\bar{f}_3\bar{a}_4 + r_1(\bar{r}_2 - \bar{r}_3)\bar{f}_4], \quad (65a)$$

$$G_{R2}^{\mu\nu(a)} = e^4 \int \frac{d^4 K}{(2\pi)^4} \frac{4K^\mu K^\nu K}{2P_3 \cdot K} [f_1(\bar{r}_2 - \bar{r}_3)\bar{r}_4 + a_1\bar{f}_2\bar{a}_4 - a_1\bar{f}_3\bar{a}_4 + a_1(\bar{r}_2 - \bar{r}_3)\bar{f}_4], \quad (65b)$$

$$G_{R3}^{\mu\nu(a)} = e^4 \int \frac{d^4 K}{(2\pi)^4} \frac{4K^\mu K^\nu K}{2P_3 \cdot K} [f_1(\bar{a}_2 - \bar{r}_3)\bar{r}_4 + r_1\bar{f}_2\bar{r}_4 - a_1\bar{f}_3\bar{a}_4 + a_1(\bar{a}_2 - \bar{r}_3)\bar{f}_4], \quad (65c)$$

$$G_{R4}^{\mu\nu(a)} = e^4 \int \frac{d^4 K}{(2\pi)^4} \frac{4K^\mu K^\nu K}{2P_3 \cdot K} [f_1(\bar{a}_2 - \bar{a}_3)\bar{r}_4 + r_1\bar{f}_2\bar{r}_4 - r_1\bar{f}_3\bar{r}_4 + a_1(\bar{a}_2 - \bar{a}_3)\bar{f}_4], \quad (65d)$$

$$G_{rara}^{\mu\nu(a)} = e^4 \int \frac{d^4 K}{(2\pi)^4} \frac{4K^\mu K^\nu K}{2P_3 \cdot K} [-f_1\bar{f}_3\bar{a}_4 + r_1(\bar{r}_2 - \bar{a}_3)\bar{a}_4 + f_1(\bar{a}_2 - \bar{r}_3)\bar{f}_4 + r_1\bar{f}_2\bar{f}_4 + a_1(\bar{a}_2 - \bar{r}_3)\bar{r}_4], \quad (65e)$$

$$G_{rraa}^{\mu\nu(a)} = e^4 \int \frac{d^4 K}{(2\pi)^4} \frac{4K^\mu K^\nu K}{2P_3 \cdot K} [r_1(\bar{a}_2 - \bar{a}_3)\bar{a}_4 + a_1(\bar{r}_2 - \bar{r}_3)\bar{r}_4 + f_1\bar{f}_2\bar{a}_4 - f_1\bar{f}_3\bar{a}_4 + f_1\bar{f}_4(\bar{r}_2 - \bar{r}_3)], \quad (65f)$$

$$G_{raar}^{\mu\nu(a)} = e^4 \int \frac{d^4 K}{(2\pi)^4} \frac{4K^\mu K^\nu K}{2P_3 \cdot K} [a_1(\bar{a}_2 - \bar{a}_3)\bar{r}_4 + r_1(\bar{r}_2 - \bar{r}_3)\bar{a}_4 + f_1\bar{f}_4(\bar{a}_2 - \bar{a}_3) + \bar{f}_2\bar{f}_4r_1 - \bar{f}_3\bar{f}_4r_1], \quad (65g)$$

where we have used the HTL approximation to write  $K_3^2 - K_2^2 = 2K \cdot P_3 + P_3^2 \approx 2K \cdot P_3$ .

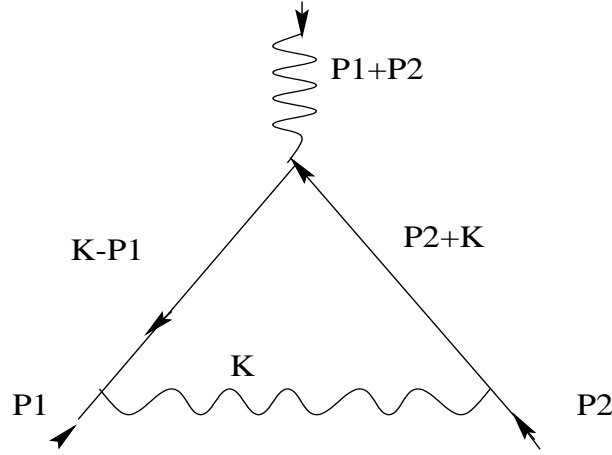


Fig. [2]: 3-point vertex in QED

The integral expressions for the 3-point vertex functions in QED are obtained from Fig. [2]. In the Feynman gauge we have

$$G_R^\mu(P_1, P_2, P_3+P_4) = e^3 \int \frac{d^4 K}{(2\pi)^4} (2K^\mu K) [a_1\bar{a}_2\bar{a}_4 + r_1\bar{r}_2\bar{r}_4 + f_1\bar{r}_2\bar{r}_4 + a_1\bar{f}_2\bar{a}_4 + a_1\bar{r}_2\bar{f}_4], \quad (66a)$$

$$G_{Ri}^\mu(P_1, P_2, P_3+P_4) = e^3 \int \frac{d^4 K}{(2\pi)^4} (2K^\mu K) [a_1\bar{a}_2\bar{a}_4 + r_1\bar{r}_2\bar{r}_4 + f_1\bar{a}_2\bar{a}_4 + r_1\bar{f}_2\bar{a}_4 + r_1\bar{r}_2\bar{f}_4], \quad (66b)$$

$$G_{Ro}^\mu(P_1, P_2, P_3+P_4) = e^3 \int \frac{d^4 K}{(2\pi)^4} (2K^\mu K) [a_1\bar{a}_2\bar{a}_4 + r_1\bar{r}_2\bar{r}_4 + f_1\bar{a}_2\bar{r}_4 + r_1\bar{f}_2\bar{r}_4 + a_1\bar{a}_2\bar{f}_4], \quad (66c)$$

$$G_F^\mu(P_1, P_2, P_3+P_4) = e^3 \int \frac{d^4 K}{(2\pi)^4} (2K^\mu K) [a_1\bar{a}_2\bar{r}_4 + r_1\bar{r}_2\bar{a}_4 + r_1\bar{f}_2\bar{f}_4 + f_1\bar{a}_2\bar{f}_4], \quad (66d)$$

$$G_{Fi}^\mu(P_1, P_2, P_3+P_4) = e^3 \int \frac{d^4 K}{(2\pi)^4} (2K^\mu K) [a_1\bar{r}_2\bar{a}_4 + r_1\bar{a}_2\bar{r}_4 + a_1\bar{f}_2\bar{f}_4 + f_1\bar{f}_2\bar{r}_4], \quad (66e)$$

$$G_{Fo}^\mu(P_1, P_2, P_3+P_4) = e^3 \int \frac{d^4 K}{(2\pi)^4} (2K^\mu K) [r_1\bar{a}_2\bar{a}_4 + a_1\bar{r}_2\bar{r}_4 + f_1\bar{f}_2\bar{a}_4 + f_1\bar{r}_2\bar{f}_4], \quad (66f)$$

where for later convenience we have chosen to write on the l.h.s.  $-(P_1+P_2) = P_3+P_4$ . Comparing (65) and (66) we obtain the following Ward identities between the vertices shown in Fig. [1a] and Fig. [2]:

$$P_{3\mu}G_{R1}^{\mu\nu(a)}(P_1, P_2, P_3, P_4) = e \left( G_{Ri}^\nu(P_1, P_2, P_3+P_4) - G_{Ri}^\nu(P_1, P_2+P_3, P_4) \right), \quad (67a)$$

$$P_{3\mu}G_{R2}^{\mu\nu(a)}(P_1, P_2, P_3, P_4) = e \left( G_R^\nu(P_1, P_2, P_3+P_4) - G_R^\nu(P_1, P_2+P_3, P_4) \right), \quad (67b)$$

$$P_{3\mu}G_{R3}^{\mu\nu(a)}(P_1, P_2, P_3, P_4) = e \left( G_{Ro}^\nu(P_1, P_2, P_3+P_4) - G_{Ro}^\nu(P_1, P_2+P_3, P_4) \right), \quad (67c)$$

$$P_{3\mu}G_{R4}^{\mu\nu(a)}(P_1, P_2, P_3, P_4) = e \left( G_{Ro}^\nu(P_1, P_2, P_3+P_4) - G_{Ro}^\nu(P_1, P_2+P_3, P_4) \right), \quad (67d)$$

$$P_{3\mu}G_{raa}^{\mu\nu(a)}(P_1, P_2, P_3, P_4) = e \left( G_F^\nu(P_1, P_2, P_3+P_4) - G_{Fo}^\nu(P_1, P_2+P_3, P_4) \right), \quad (67e)$$

$$P_{3\mu}G_{raar}^{\mu\nu(a)}(P_1, P_2, P_3, P_4) = e \left( G_F^\nu(P_1, P_2, P_3+P_4) - G_F^\nu(P_1, P_2+P_3, P_4) \right), \quad (67f)$$

$$P_{3\mu}G_{rraa}^{\mu\nu(a)}(P_1, P_2, P_3, P_4) = e \left( G_{Fo}^\nu(P_1, P_2, P_3+P_4) - G_{Fo}^\nu(P_1, P_2+P_3, P_4) \right). \quad (67g)$$

Similarly one can obtain the Ward identities satisfied by the diagrams in Fig. [1b] and Fig. [2]:

$$P_{3\mu}G_{R1}^{\mu\nu(b)}(P_1, P_2, P_3, P_4) = e \left( G_{Ri}^\nu(P_1+P_3, P_2, P_4) - G_{Ri}^\nu(P_1, P_2, P_3+P_4) \right), \quad (68a)$$

$$P_{3\mu}G_{R2}^{\mu\nu(b)}(P_1, P_2, P_3, P_4) = e \left( G_R^\nu(P_1+P_3, P_2, P_4) - G_R^\nu(P_1, P_2, P_3+P_4) \right), \quad (68b)$$

$$P_{3\mu}G_{R3}^{\mu\nu(b)}(P_1, P_2, P_3, P_4) = e \left( G_{Ro}^\nu(P_1+P_3, P_2, P_4) - G_{Ro}^\nu(P_1, P_2, P_3+P_4) \right), \quad (68c)$$

$$P_{3\mu}G_{R4}^{\mu\nu(b)}(P_1, P_2, P_3, P_4) = e \left( G_{Ri}^\nu(P_1+P_3, P_2, P_4) - G_{Ro}^\nu(P_1, P_2, P_3+P_4) \right), \quad (68d)$$

$$P_{3\mu}G_{raa}^{\mu\nu(b)}(P_1, P_2, P_3, P_4) = e \left( G_F^\nu(P_1+P_3, P_2, P_4) - G_F^\nu(P_1, P_2, P_3+P_4) \right), \quad (68e)$$

$$P_{3\mu}G_{raar}^{\mu\nu(b)}(P_1, P_2, P_3, P_4) = -e G_F^\nu(P_1, P_2, P_3+P_4), \quad (68f)$$

$$P_{3\mu}G_{rraa}^{\mu\nu(b)}(P_1, P_2, P_3, P_4) = e \left( G_{Fo}^\nu(P_1+P_3, P_2, P_4) - G_{Fo}^\nu(P_1, P_2, P_3+P_4) \right). \quad (68g)$$

By combining (67) and (68) one obtains the following HTL Ward identities between the 3- and 4-point vertex functions in QED in the RTF:

$$P_{3\mu}G_{R1}^{\mu\nu}(P_1, P_2, P_3, P_4) = e \left( G_{Ri}^\nu(P_1+P_3, P_2, P_4) - G_{Ri}^\nu(P_1, P_2+P_3, P_4) \right), \quad (69a)$$

$$P_{3\mu}G_{R2}^{\mu\nu}(P_1, P_2, P_3, P_4) = e \left( G_R^\nu(P_1+P_3, P_2, P_4) - G_R^\nu(P_1, P_2+P_3, P_4) \right), \quad (69b)$$

$$P_{3\mu}G_{R3}^{\mu\nu}(P_1, P_2, P_3, P_4) = e \left( G_R^\nu(P_1+P_3, P_2, P_4) - G_{Ro}^\nu(P_1, P_2+P_3, P_4) \right), \quad (69c)$$

$$P_{3\mu}G_{R4}^{\mu\nu}(P_1, P_2, P_3, P_4) = e \left( G_{Ro}^\nu(P_1+P_3, P_2, P_4) - G_{Ri}^\nu(P_1, P_2+P_3, P_4) \right), \quad (69d)$$

$$P_{3\mu}G_{raa}^{\mu\nu}(P_1, P_2, P_3, P_4) = e \left( G_F^\nu(P_1+P_3, P_2, P_4) - G_{Fo}^\nu(P_1, P_2+P_3, P_4) \right), \quad (69e)$$

$$P_{3\mu}G_{raar}^{\mu\nu}(P_1, P_2, P_3, P_4) = -e G_F^\nu(P_1, P_2+P_3, P_4), \quad (69f)$$

$$P_{3\mu}G_{rraa}^{\mu\nu}(P_1, P_2, P_3, P_4) = e \left( G_{Fo}^\nu(P_1+P_3, P_2, P_4) - G_{Fo}^\nu(P_1, P_2+P_3, P_4) \right). \quad (69g)$$

Notice that in equilibrium the last equation gives simply  $0 = 0$  (see (49) and (53)). These results are structurally similar to the zero temperature Ward identity [29] and to the Ward identities between the retarded 3- and 4-point HTL vertices in QCD obtained within the imaginary time formalism [8] or from kinetic theory [10].

## VII. EXTENSION TO NON-EQUILIBRIUM SITUATIONS

The HTL method has been widely used in qualitative studies of the QGP and in other explicit calculations at finite temperature [5]. This powerful method was derived within the ITF for equilibrium field theory, and this is where its range of applicability can be clearly defined [4,5,8]: HTL resummation is required and applicable for the study of soft processes in a weakly interacting plasma, with momentum scale  $p \sim gT \ll T$  ( $g \ll 1$ ) much below the typical thermal or “hard” momenta in the medium. Realistic physical systems, on the other hand, are frequently out of equilibrium, which means that calculations must be carried out in the RTF. As long as the local momentum distribution  $f(x, p)$

doesn't deviate too strongly from a thermal one, and can still be roughly characterized by a parameter  $T$  which gives the scale for the typical momenta at point  $x$ , a similar “hard loop” (HL) resummation scheme should be applicable for the study of the dynamics of soft modes ( $p \sim gT \ll T$ ) in a weakly interacting ( $g \ll 1$ ) non-equilibrium system [28]. This approach is expected to be reliable for equilibration processes requiring momentum exchanges which happen slowly, on a time scale  $\tau \sim (g^2 T)^{-1} \gg 1/p^0$ . This reasoning does not apply to arbitrary non-equilibrium situations, but only to plasma states which are sufficiently close to global thermal equilibrium; on the other hand, deviations from chemical equilibrium can be arbitrarily strong without invalidating the scheme.

In this section we discuss the generalization of our results to this particular type of non-equilibrium scenarios. Since we have used the Keldysh or closed time path contour, the procedure is straightforward. Equations (1) and (2) can be used in non-equilibrium situations by replacing the  $x$ -independent equilibrium Bose-Einstein and Fermi-Dirac distributions by non-equilibrium distributions (Wigner functions)  $f_B(x, p)$  and  $f_F(x, p)$  which depend on the space-time coordinate and the four momenta [21]. Equations (6) and (7) remain valid for bare propagators, with the equilibrium distribution functions ( $n_B, n_F$ ) replaced by the non-equilibrium ones ( $f_B, f_F$ ), but the last equations in each of (6) and (7), (i.e. the fluctuation-dissipation theorem which reflects the KMS condition), no longer hold for full propagators [28].

Equations (30) give the spectral representations of the seven 4-point functions (10) in equilibrium. These expressions remain valid out of equilibrium since the KMS condition was not used in their derivation. Out of equilibrium there are eight more 4-point vertex functions ( $G_{arr}, G_{rarr}, G_{rrar}, G_{rrra}, G_{arar}, G_{aarr}, G_{arra}$  and  $G_{rrrr}$ ) with similar spectral representations. They can be derived using the same methods as those given in Sec. III.

The results in Secs. IV and V can be generalized to non-equilibrium situations by simply replacing in (44) and (48) the Bose-Einstein and Fermi-Dirac distributions  $n_B(p^0)$  and  $n_F(p^0)$  by non-equilibrium Wigner functions  $f_B(x, p)$  and  $f_F(x, p)$ . The thermal mass  $m_\beta$  in (44) and the factors  $c_\beta, d_\beta$  in (48) become functions of  $x, m(x), c(x), d(x)$ , and it is only in the special case of thermal equilibrium that  $c = 0$  as obtained in (49). These generalized results correspond to the “hard loop” (HL) approximation in slightly off-equilibrium plasmas and are applicable in the situations discussed at the beginning of this section. We have shown that the 7 components of the 4-point function given in (10) correspond to 5 spectral densities which degenerate in the HL approximation to a single real function. This result remains valid out of equilibrium, where the KMS conditions do not hold. The eight additional 4-point functions which must be included out of equilibrium will involve more spectral functions, but in the HL approximation it is straightforward to show that they degenerate to the same HTL spectral density (55), with the thermal mass  $m_\beta$  replaced by the generalized mass  $m(x)$ .

The one-loop Ward identities in Sec. VI were obtained without explicitly doing any momentum integrals; the result thus holds independently of the form of the distribution functions (which enter through the functions  $f_i, \bar{f}_i$  in (65) and (66)). Out of equilibrium there will be additional Ward identities for the eight additional vertex functions which can be derived in the same way. For example, the Ward identities that correspond to the three functions  $G_{aarr}, G_{arra}, G_{arar}$  have been calculated, and they have the same form as those obtained in (69 e,f,g).

## VIII. CONCLUSIONS

We have studied the 4-point vertex functions in the Keldysh formulation of real-time thermal field theory [22]. This formalism has recently gained increased popularity because it avoids the need for analytical continuation associated with the imaginary time formalism, and it allows for a generalization to non-equilibrium situations. Starting from the largest time and smallest time equations which relate the 16 components of the 4-point real-time vertex function, we have derived spectral integral representations for the 7 retarded-advanced 4-point functions (10). We have explicitly calculated these 7 functions for hot QED at 1-loop order in the HTL approximation, using the Keldysh representation. In particular, we have demonstrated the usefulness of this representation for the calculation of many-point functions and showed how terms with high powers of the distribution functions cancel explicitly before any momentum integrations are done. The fully retarded vertex functions are found to be linear in the distribution functions [27]. In the HTL approximation, they have the same structure as their QCD counterparts which were derived in the ITF [4,30] as well as from kinetic theory [10]. We have also calculated the three mixed retarded-advanced 4-point functions which are needed for a complete description of the real-time 4-point vertex and which have not previously appeared in the literature. They are quadratic in the distribution functions. One of them ( $G_{rraa}$ ) was found to vanish in thermal equilibrium, while the other 4-point functions are all proportional to  $T^2$ .

We have derived spectral integral representations for the 7 retarded-advanced 4-point functions (10). The spectral densities were calculated explicitly for hot QED in the HTL approximation and found in this case to degenerate to a single real spectral function. Its trace over the Lorentz indices vanishes, and it is transverse with respect to all 4 external momenta. It obeys a simple sum rule with the correspondingly approximated 3-point spectral density.

By contracting the 7 retarded-advanced 4-point functions (10) for QED in the HTL approximation with one of the photon momenta we have derived one-loop Ward identities. This calculation was done without doing any momentum integrations, by comparing the integrands of the contracted HTL 4-point vertices with those of the HTL 3-point vertices. The resulting set of real-time Ward identities at finite temperature generalizes the zero temperature Ward identity and can be compared with the HTL Ward identity from the ITF and from kinetic theory. Due to the matrix form of the real-time thermal Green functions, the Ward identities have a more complex structure: one finds a whole class of finite temperature Ward identities which relate retarded-advanced 4-point functions to retarded-advanced 3-point vertex functions. If either the ingoing or the outgoing fermion leg has the largest time, the Ward identity involves only one kind of retarded-advanced 3-point vertex functions, and the right hand side vanishes when the contracted photon momentum ( $P_3$ ) goes to zero. If one of the photon legs has the largest time, two different retarded-advanced 3-point functions are involved, and the right hand side no longer vanishes (Eqs. (69c-f)); the corresponding component of the 4-point vertex is thus singular in the zero-momentum limit  $P_3 \rightarrow 0$  [31]. Similar features were found for the Ward identities relating the HTL 3- and 2-point functions in hot QED [20].

Our Ward identities are not general, in the sense that they were not directly derived by functional methods from the RTF path integral. However, in the case of the 3-point functions it is known that the one-HTL Ward identities [20] are identical in structure with those satisfied by the exact vertex functions [32]. We therefore expect the same to be true in the present case.

Finally, we have discussed the generalization of our results to certain classes of “moderately non-equilibrium” situations (Sec. VII) in which a generalized HTL approximation (“hard loop approximation”) can be applied. Out of equilibrium the number of independent 4-point functions is larger, but in the HL approximation the spectral functions have the same structure as in equilibrium. All of the nice features of equilibrium HTLs persist in such “moderately non-equilibrium” situations.

## ACKNOWLEDGMENTS

We are grateful for interesting discussions with M. Thoma. This work was supported by the National Natural Science Foundation of China (NSFC), the Deutsche Forschungsgemeinschaft (DFG), the Bundesministerium für Bildung und Forschung (BMBF), the Gesellschaft für Schwerionenforschung (GSI), and the Natural Sciences and Engineering and Research Council of Canada (NSERC).

- 
- [1] N.P. Landsman and Ch.G. van Weert, Phys. Rep. **145**, 141 (1987).
  - [2] J.I. Kapusta, *Finite Temperature Field Theory* (Cambridge University Press, 1989).
  - [3] M. LeBellac, *Thermal Field Theory* (Cambridge University Press, 1996).
  - [4] E. Braaten and R.D. Pisarski, Nucl. Phys. **B337**, 569 (1990); and **B339**, 310 (1990).
  - [5] M.H. Thoma, in *Quark-Gluon Plasma 2*, p. 51, ed. by R.C. Hwa (World Scientific, Singapore, 1996).
  - [6] U. Heinz, Ann. Phys. (N.Y.) **168**, 48 (1986).
  - [7] J. Frenkel and J.C. Taylor, Nucl. Phys. **B334**, 199 (1990).
  - [8] E. Braaten and R.D. Pisarski, Phys. Rev. D **45**, 1827 (1992).
  - [9] R. Jackiw, V.P. Nair, Phys. Rev. D **48**, 4991 (1993).
  - [10] J.-P. Blaizot and E. Iancu, Phys. Rev. Lett. **70**, 3376 (1993); Nucl. Phys. **B417**, 608 (1994).
  - [11] P.F. Kelly, Q. Liu, C. Lucchesi, and C. Manuel, Phys. Rev. Lett. **72**, 3461 (1994).
  - [12] S. Jeon, Phys. Rev. D **47**, 4586 (1993); and **52**, 3591 (1995).
  - [13] E. Wang, U. Heinz, and X.-F. Zhang, Phys. Rev. D **53**, 5978 (1996).
  - [14] R. Kobes and G.W. Semenoff, Nucl. Phys. **B260**, 714 (1985); and **B272**, 329 (1986).
  - [15] R. Kobes, Phys. Rev. D **43**, 1269 (1991).
  - [16] T.S. Evans, Phys. Lett. B **249**, 286 (1990); **252**, 108 (1990); and Nucl. Phys. **B374**, 340 (1992).
  - [17] J.C. Taylor, Phys. Rev. D **47** (1993) 725
  - [18] J.C. Taylor, Phys. Rev. D **48**, 958 (1993).
  - [19] M.E. Carrington and U. Heinz, Eur. Phys. J. **C1**, 619 (1998).
  - [20] Hou Defu and U. Heinz, Eur. Phys. J. **C4**, 129 (1998); and **C7**, 101 (1999).
  - [21] K.-C. Chou, Z.-B. Su, B.-L. Hao, and L. Yu, Phys. Rep. **118**, 1 (1985).
  - [22] L.V. Keldysh, Zh. Eksp. Teor. Fiz. **47**, 1515 (1964) [JETP **20**, 1018 (1965)].
  - [23] P.A. Henning, Phys. Rep. **253**, 235 (1995).

- [24] R. Kobes, Phys. Rev. D **42**, 562 (1990).
- [25] E. Wang and U. Heinz, hep-th/9809016.
- [26] Hou Defu, E. Wang, and U. Heinz, J. Phys. G **24**, 1861 (1998).
- [27] R. Baier, B. Pire, and D. Schiff, Z. Phys. C **51**, 581 (1991); P. Aurenche, E. Petitgirard and T.R. Gaztelurrutia, Phys. Lett. B **297**, 337 (1992).
- [28] M. Carrington, Hou Defu, and M.H. Thoma, Phys. Rev. D **58**, 085025 (1998); Eur. Phys. J. **C7**, 347 (1999).
- [29] J.C. Ward, Phys. Rev. **77**, 293 (1950); Y. Takahashi, Nuovo Cimento **6**, 340 (1957).
- [30] J. Frenkel and J.C. Taylor, Nucl. Phys. B **374**, 156 (1992).
- [31] We thank D. Boyanovsky and S.-Y. Wang for pointing this out. They observed that at  $p=p'$  the r.h.s. of the Ward identity (39c) in the second reference [20] develops a pinch singularity as can be seen from Eq. (38b) in the same paper. Its physical interpretation is unclear to us.
- [32] J.C. D'Olivo, M. Torres, and E. Tútuti, Phys. Rev. D **55**, 3859 (1997).

## FOUR-POINT SPECTRAL FUNCTIONS AND WARD IDENTITIES IN HOT QED

Hou Defu<sup>1,2,3</sup>, M.E. Carrington<sup>1,3</sup>, R. Kobes<sup>1,4</sup>, and U. Heinz<sup>5</sup>

<sup>1</sup>Winnipeg Institute for Theoretical Physics, Winnipeg, Manitoba

<sup>2</sup>Institute of Particle Physics, Huazhong Normal University, 430070 Wuhan, China

<sup>3</sup>Physics Department, Brandon University, Brandon, Manitoba, R7A 6A9, Canada

<sup>4</sup>Physics Department, University of Winnipeg, Winnipeg, Manitoba, R3B 2E9, Canada

<sup>5</sup>Theoretical Physics Division, CERN, CH-1211 Geneva 23, Switzerland

### ABSTRACT

We derive spectral representations for the different components of the 4-point function at finite temperature in the real time formalism in terms of five real spectral densities. We explicitly calculate all these functions in QED in the hard thermal loop approximation. The Ward identities obeyed by the 1-loop 3- and 4-point functions in real time and their spectral functions are derived. We compare our results with those derived previously in the imaginary-time formalism for retarded functions in hot QCD, and we discuss the generalization of our results to non-equilibrium situations.

*Submitted to Physical Review D*



# Four-Point Spectral Functions and Ward Identities in Hot QED

Hou Defu<sup>1,2,3</sup>, M.E. Carrington<sup>1,3</sup>, R. Kobes<sup>1,4</sup>, and U. Heinz<sup>5,\*</sup>

<sup>1</sup>*Winnipeg Institute for Theoretical Physics, Winnipeg, Manitoba*

<sup>2</sup>*Institute of Particle Physics, Huazhong Normal University, 430070 Wuhan, China*

<sup>3</sup>*Physics Department, Brandon University, Brandon, Manitoba, R7A 6A9, Canada*

<sup>4</sup>*Physics Department, University of Winnipeg, Winnipeg, Manitoba, R3B 2E9, Canada*

<sup>5</sup>*Theoretical Physics Division, CERN, CH-1211 Geneva 23, Switzerland*

(November 26, 1999)

We derive spectral representations for the different components of the 4-point function at finite temperature in the real time formalism in terms of five real spectral densities. We explicitly calculate all these functions in QED in the hard thermal loop approximation. The Ward identities obeyed by the 1-loop 3- and 4-point functions in real time and their spectral functions are derived. We compare our results with those derived previously in the imaginary-time formalism for retarded functions in hot QCD, and we discuss the generalization of our results to non-equilibrium situations.

PACS numbers: 11.10Wx, 11.15Tk, 11.55Fv

## I. INTRODUCTION

One of the most significant advances in quantum field theory at finite temperature [1–3] is the effective perturbation theory of Braaten and Pisarski [4,5] which is based on the resummation of hard thermal loops (HTLs). HTLs were originally obtained by computing one-loop diagrams in the imaginary time formulation of finite temperature field theory. HTLs are ultraviolet finite, gauge invariant and satisfy simple Ward identities [6–9]. These remarkable properties have been traced to the fact that HTLs describe simple semiclassical physics [6,10,11]. In particular, the HTLs can be derived from a set of classical kinetic equations [6,10] as well as from a non-local effective Lagrangian [8]. The computation of HTLs is fairly technical because of their non-trivial momentum and energy dependence, but can be simplified by using the Ward identities [4].

The analytical structure of Green functions at zero or non-zero temperature, in the imaginary or real-time formulations, is controlled by their spectral densities, combined with asymptotic boundary conditions. At finite temperature the spectral functions can also be directly related to transport coefficients [12,13]. The study of spectral functions helps us to understand the quasi-particle structure of a field theory and to identify the microscopic processes underlying the dynamics. But Green functions and their spectral functions are not easy quantities to evaluate perturbatively at non-zero temperature, especially for many-point functions. The two-point functions and their spectral densities have been widely studied and applied to quark gluon plasma (QGP) investigations [14,3,5,12]. Our knowledge about many-point spectral densities is still much less comprehensive [15–20]. The spectral representations of 3-point functions for self-interacting scalar fields were discussed in Refs. [15,16,19,20]. In [18] 3- and 4-point spectral densities for pure gluon dynamics were calculated in the HTL approximation using the imaginary time formalism (ITF) [4], and in the same approximation the 3-point spectral density in QED has been calculated within the real time formalism (RTF) [20].

The popularity of the RTF is diminished by the technical complications resulting from the doubling of degrees of freedom [21]. However, in the ITF, one has to perform an analytic continuation of the imaginary external energy variables to the real axis, which is avoided in the RTF. In addition, the ITF is restricted to equilibrium situations, while the RTF can be extended to investigate non-equilibrium systems [21–23].

In this paper we study 4-point functions in QED using the real-time formalism. We adopt the Keldysh or closed time path (CTP) contour [22]. In Sec. II we introduce the Keldysh representation. The spectral representations of the 4-point functions is derived in Sec. III. In Sec. IV we use the Keldysh representation to calculate the 4-point HTL vertex functions in hot QED. The 4-point spectral densities in the HTL approximation are extracted in Sec. V and shown to degenerate to a single real spectral function. In Sec. VI we derive real-time Ward identities between the 3-

---

\*On leave from Institut für Theoretische Physik, Universität Regensburg, D-93040 Regensburg, Germany.

and 4-point HTLs and their spectral functions. The generalization of our results to certain types of non-equilibrium situations is discussed in Sec. VII, while Sec. VIII gives a summary of our results.

## II. KELDYSH REPRESENTATION

We will use the Keldysh representation [21,22] of the real-time formalism (RTF) throughout this paper. In this representation the single-particle propagator for free bosons has in momentum space the form [21,22]

$$D(K) = \begin{pmatrix} \frac{1}{K^2 - m^2 + i\epsilon} & 0 \\ 0 & \frac{-1}{K^2 - m^2 - i\epsilon} \end{pmatrix} - 2\pi i \delta(K^2 - m^2) \begin{pmatrix} n_B(k_0) & \theta(-k_0) + n_B(k_0) \\ \theta(k_0) + n_B(k_0) & n_B(k_0) \end{pmatrix} \quad (1)$$

where  $K = (k_0, \mathbf{k})$ ,  $k = |\mathbf{k}|$ ,  $\theta$  denotes the step function, and the equilibrium distribution function is given by  $n_B(k_0) = 1/[\exp(|k_0|/T) - 1]$ . For fermions the bare propagator can be written as

$$S(K) = (\not{K} + m) \left[ \begin{pmatrix} \frac{1}{K^2 - m^2 + i\epsilon} & 0 \\ 0 & \frac{-1}{K^2 - m^2 - i\epsilon} \end{pmatrix} + 2\pi i \delta(K^2 - m^2) \begin{pmatrix} n_F(k_0) & -\theta(-k_0) + n_F(k_0) \\ \theta(k_0) - n_F(k_0) & n_F(k_0) \end{pmatrix} \right], \quad (2)$$

where the Fermi-Dirac distribution is given by  $n_F(k_0) = 1/[\exp(|k_0|/T) + 1]$ . The components of these propagators are not independent, but fulfill the relation

$$G_{11} - G_{12} - G_{21} + G_{22} = 0, \quad (3)$$

where  $G$  stands for  $D$  or  $S$ , respectively.

By an orthogonal transformation of these  $2 \times 2$  matrices one arrives at the representation of the propagators in terms of advanced and retarded propagators which was first introduced by Keldysh [22]. The three nonvanishing components of this representation are [21]

$$\begin{aligned} G_R &= G_{11} - G_{12}, \\ G_A &= G_{11} - G_{21}, \\ G_F &= G_{11} + G_{22}. \end{aligned} \quad (4)$$

The inverted relations read

$$\begin{aligned} G_{11} &= \frac{1}{2} (G_F + G_A + G_R), \\ G_{12} &= \frac{1}{2} (G_F + G_A - G_R), \\ G_{21} &= \frac{1}{2} (G_F - G_A + G_R), \\ G_{22} &= \frac{1}{2} (G_F - G_A - G_R). \end{aligned} \quad (5)$$

The relations (3–5) also hold for full propagators.

Using (1) and (2) in (4), the free propagators are given in the Keldysh representation by

$$\begin{aligned} D_R(K) &= \frac{1}{K^2 - m^2 + i \operatorname{sgn}(k_0)\epsilon}, \\ D_A(K) &= \frac{1}{K^2 - m^2 - i \operatorname{sgn}(k_0)\epsilon}, \\ D_F(K) &= (1 + 2n_B(k_0)) \operatorname{sgn}(k_0) (D_R(K) - D_A(K)) = -2\pi i (1 + 2n_B(k_0)) \delta(K^2 - m^2) \end{aligned} \quad (6)$$

for bosons and

$$\begin{aligned} S_R(K) &= \frac{\not{K} + m}{K^2 - m^2 + i \operatorname{sgn}(k_0)\epsilon} = (\not{K} + m) \bar{D}_R(K), \\ S_A(K) &= \frac{\not{K} + m}{K^2 - m^2 - i \operatorname{sgn}(k_0)\epsilon} = (\not{K} + m) \bar{D}_A(K), \\ S_F(K) &= (1 - 2n_F(k_0)) \operatorname{sgn}(k_0) (S_R(K) - S_A(K)) \\ &= -2\pi i (\not{K} + m) (1 - 2n_F(k_0)) \delta(K^2 - m^2) = (\not{K} + m) \bar{D}_F(K) \end{aligned} \quad (7)$$

for fermions, where the last equation in each of (6) and (7) is a consequence of the dissipation-fluctuation theorem. Although  $\bar{D}_{A,R} = D_{A,R}$  we keep the bar in our notation to more easily recognize fermion and boson propagators in the calculations below.

### III. SPECTRAL REPRESENTATION OF THE 4-POINT VERTEX

In this section we briefly review some useful relations among the different thermal components of the 4-point functions, and we derive their spectral representations. Some of these relations have already been reported in the literature [14–16,24] using different notation. We discuss these results at the end of this section. For any 1PI four-point function we define the four incoming external momenta as  $P_1, P_2, P_3$ , and  $P_4 = -(P_1+P_2+P_3)$ . In this section we suppress all indices except Keldysh indices.

#### A. Largest and smallest time equations

If  $t_4$  is the largest time argument, one can obtain the “largest time equations” [14,15,24]:

$$\theta_{43} \theta_{32} \theta_{21} (G_{abc1} + G_{abc2}) = \theta_{43} \theta_{31} \theta_{12} (G_{abc1} + G_{abc2}) = 0, \quad (8a)$$

$$\theta_{42} \theta_{23} \theta_{31} (G_{abc1} + G_{abc2}) = \theta_{42} \theta_{23} \theta_{13} (G_{abc1} + G_{abc2}) = 0, \quad (8b)$$

$$\theta_{41} \theta_{13} \theta_{32} (G_{abc1} + G_{abc2}) = \theta_{41} \theta_{12} \theta_{23} (G_{abc1} + G_{abc2}) = 0, \quad (8c)$$

$$\theta_{32} \theta_{21} \theta_{14} (G_{ab1c} + G_{ab2c}) = \theta_{31} \theta_{12} \theta_{24} (G_{ab1c} + G_{ab2c}) = 0, \quad (8d)$$

$$\theta_{23} \theta_{34} \theta_{41} (G_{a1bc} + G_{a2bc}) = \theta_{24} \theta_{43} \theta_{31} (G_{a1bc} + G_{a2bc}) = 0, \quad (8e)$$

$$\theta_{13} \theta_{32} \theta_{24} (G_{1abc} + G_{2abc}) = \theta_{12} \theta_{23} \theta_{34} (G_{1abc} + G_{2abc}) = 0, \quad (8f)$$

where  $a, b, c$  can be either 1 or 2, and  $\theta_{ij} \equiv \theta(t_i - t_j)$  is the step function.

By tilde conjugation (which replaces time ordering with anti-time ordering [21,23]) one obtains equations of the form:

$$\theta_{12} \theta_{23} \theta_{34} (\tilde{G}_{abc1} + \tilde{G}_{abc2}) = \theta_{13} \theta_{32} \theta_{24} (\tilde{G}_{abc1} + \tilde{G}_{abc2}) = 0, \quad (9a)$$

$$\theta_{41} \theta_{12} \theta_{23} (\tilde{G}_{ab1c} + \tilde{G}_{ab2c}) = \theta_{42} \theta_{21} \theta_{13} (\tilde{G}_{ab1c} + \tilde{G}_{ab2c}) = 0, \quad (9b)$$

$$\theta_{14} \theta_{43} \theta_{32} (\tilde{G}_{a1bc} + \tilde{G}_{a2bc}) = \theta_{13} \theta_{34} \theta_{42} (\tilde{G}_{a1bc} + \tilde{G}_{a2bc}) = 0, \quad (9c)$$

$$\theta_{42} \theta_{23} \theta_{31} (\tilde{G}_{1abc} + \tilde{G}_{2abc}) = \theta_{43} \theta_{32} \theta_{21} (\tilde{G}_{1abc} + \tilde{G}_{2abc}) = 0, \quad (9d)$$

Eqs. (8) and (9) are the analogues of the “largest time equations” and “smallest time equations”, respectively, of Ref. [14]. They will be used extensively in the derivation of the spectral representations below. Their generalization to arbitrary  $n$ -point functions is straightforward.

#### B. Derivation of spectral representations

One can construct the “retarded–advanced” vertex functions from the sixteen components of the real-time 4-point function as in [19,21]. The KMS conditions allows to reduce them to the following seven combinations [25,26]:

$$G_{raaa} = G_{1111} + G_{1211} + G_{1121} + G_{1112} + G_{1122} + G_{1221} + G_{1212} + G_{1222}, \quad (10a)$$

$$G_{araa} = G_{1111} + G_{2111} + G_{1121} + G_{1112} + G_{1122} + G_{2121} + G_{2112} + G_{2122}, \quad (10b)$$

$$G_{aara} = G_{1111} + G_{2111} + G_{1211} + G_{1112} + G_{1212} + G_{2211} + G_{2112} + G_{2212}, \quad (10c)$$

$$G_{aaar} = G_{1111} + G_{2111} + G_{1211} + G_{1121} + G_{1221} + G_{2211} + G_{2121} + G_{2221}, \quad (10d)$$

$$G_{rara} = G_{1111} + G_{1211} + G_{1112} + G_{1212} + G_{2121} + G_{2122} + G_{2221} + G_{2222}, \quad (10e)$$

$$G_{rraa} = G_{1111} + G_{1112} + G_{1121} + G_{1122} + G_{2211} + G_{2212} + G_{2221} + G_{2222}, \quad (10f)$$

$$G_{raar} = G_{1111} + G_{1121} + G_{1211} + G_{1221} + G_{2112} + G_{2122} + G_{2212} + G_{2222}. \quad (10g)$$

It is straightforward to show that the first four are the standard retarded vertex functions

$$G_{raaa} = G_{R1}; \quad G_{araa} = G_{R2}; \quad G_{aara} = G_{R3}; \quad G_{aaar} = G_{R4}. \quad (11)$$

The last three we will call “mixed retarded-advanced” functions.

There are eight other vertices which one can obtain from (10) using the KMS conditions [25,26]. We write down only the three which we need:

$$G_{arar} = G_{1111} + G_{1121} + G_{2111} + G_{2121} + G_{1212} + G_{1222} + G_{2212} + G_{2222}, \quad (12a)$$

$$G_{arra} = G_{1111} + G_{1112} + G_{2111} + G_{2112} + G_{1221} + G_{1222} + G_{2221} + G_{2222}, \quad (12b)$$

$$G_{aarr} = G_{1111} + G_{1211} + G_{2111} + G_{2211} + G_{1122} + G_{1222} + G_{2122} + G_{2222}. \quad (12c)$$

We can re-express these vertices in terms of spectral functions by making use of various properties of theta functions. We will use

$$\theta_{12} + \theta_{21} = 1, \quad \theta_{12}\theta_{21} = 0, \quad \theta_{23}\theta_{34}\theta_{24} = \theta_{23}\theta_{34}. \quad (13)$$

(i) We begin with  $G_{R1}$ . We rewrite  $G_{R1}$  as

$$G_{R1} = (\theta_{23} + \theta_{32})(\theta_{34} + \theta_{43})(\theta_{24} + \theta_{42})G_{R1}. \quad (14)$$

Inserting the identities

$$\theta_{13}G_{R1} = \theta_{12}G_{R1} = \theta_{14}G_{R1} = G_{R1} \quad (15)$$

into (14) we obtain

$$\begin{aligned} G_{R1} &= \theta_{12}\theta_{23}\theta_{34}G_{R1} + \theta_{12}\theta_{24}\theta_{43}G_{R1} + \theta_{14}\theta_{42}\theta_{23}G_{R1} \\ &\quad + \theta_{14}\theta_{43}\theta_{32}G_{R1} + \theta_{13}\theta_{34}\theta_{42}G_{R1} + \theta_{13}\theta_{32}\theta_{24}G_{R1}. \end{aligned} \quad (16)$$

Using the identities

$$\begin{aligned} \theta(1ijk)G_{R2} &= \theta_{1i}\theta_{ij}\theta_{jk}G_{R2} = 0, \\ \theta(1ijk)G_{R3} &= \theta_{1i}\theta_{ij}\theta_{jk}G_{R3} = 0, \\ \theta(1ijk)G_{R4} &= \theta_{1i}\theta_{ij}\theta_{jk}G_{R4} = 0, \quad (i, j, k = 2, 3, 4) \end{aligned} \quad (17)$$

which result from conflicting  $\theta$ -functions, we have

$$\begin{aligned} G_{R1} &= [\theta(1234) + \theta(1243) + \theta(1324) + \theta(1342) + \theta(1423) + \theta(1432)] (G_{R1} - G_{R2} + G_{R3} - G_{R4}) \\ &= [\theta(1234) + \theta(1243) + \theta(1324) + \theta(1342) + \theta(1423) + \theta(1432)] \rho_{12} \end{aligned} \quad (18)$$

with

$$\begin{aligned} \rho_{12} &= G_{R1} - G_{R2} + G_{R3} - G_{R4} \\ &= G_{1211} - G_{2122} + 2(G_{1212} - G_{2121}) + G_{1112} - G_{2221} + G_{1222} - G_{2111} + G_{2212} - G_{1121}. \end{aligned} \quad (19)$$

(ii) For  $G_{R2}$ ,  $G_{R3}$  and  $G_{R4}$  one proceeds similarly and obtains

$$G_{R2} = [\theta(2134) + \theta(2143) + \theta(2314) + \theta(2341) + \theta(2413) + \theta(2431)](-\rho_{12}), \quad (20a)$$

$$G_{R3} = [\theta(3124) + \theta(3142) + \theta(3214) + \theta(3241) + \theta(3412) + \theta(3421)]\rho_{12}, \quad (20b)$$

$$G_{R4} = [\theta(4123) + \theta(4132) + \theta(4213) + \theta(4231) + \theta(4312) + \theta(4321)](-\rho_{12}). \quad (20c)$$

(iii) The procedure for the mixed retarded-advanced four-point functions is similar. We write

$$G_{rraa} = (\theta_{12} + \theta_{21})(\theta_{14} + \theta_{41})(\theta_{23} + \theta_{32})(\theta_{34} + \theta_{43})(\theta_{24} + \theta_{42})G_{rraa} \quad (21)$$

and use

$$\begin{aligned} \theta(3ijk)G_{rraa} &= 0, \quad i, j, k = 1, 2, 4, \\ \theta(4ijk)G_{rraa} &= 0, \quad i, j, k = 1, 3, 4, \end{aligned} \quad (22)$$

to obtain

$$G_{rraa} = [\theta(1234) + \theta(1243) + \theta(1324) + \theta(1342) + \theta(1423) + \theta(1432) \\ + \theta(2134) + \theta(2143) + \theta(2314) + \theta(2341) + \theta(2413) + \theta(2431)] G_{rraa}. \quad (23)$$

Using the identities

$$\begin{aligned} \theta(1ijk)\tilde{G}_{rraa} &= 0, \quad i, j, k = 2, 3, 4, \\ \theta(2ijk)\tilde{G}_{rraa} &= 0, \quad i, j, k = 1, 3, 4 \end{aligned} \quad (24)$$

allows us to write

$$G_{rraa} = [\theta(1234) + \theta(1243) + \theta(1324) + \theta(1342) + \theta(1423) + \theta(1432) \\ + \theta(2134) + \theta(2143) + \theta(2314) + \theta(2341) + \theta(2413) + \theta(2431)] \rho_3 \quad (25)$$

with

$$\rho_3 = G_{rraa} - \tilde{G}_{rraa}. \quad (26)$$

Analogously, we can derive

$$G_{rara} = [\theta(1234) + \theta(1243) + \theta(1324) + \theta(1342) + \theta(1423) + \theta(1432) \\ + \theta(3124) + \theta(3142) + \theta(3214) + \theta(3241) + \theta(3412) + \theta(3421)] \rho_4 \quad (27a)$$

$$G_{raar} = [\theta(1234) + \theta(1243) + \theta(1324) + \theta(1342) + \theta(1423) + \theta(1432) \\ + \theta(4123) + \theta(4132) + \theta(4213) + \theta(4231) + \theta(4321) + \theta(4312)] \rho_5 \quad (27b)$$

where

$$\rho_4 = G_{rara} - \tilde{G}_{rara} \quad (28a)$$

$$\rho_5 = G_{raar} - \tilde{G}_{raar} \quad (28b)$$

Using the Fourier integral representation of the  $\theta$  function,

$$\theta_{ij} = -\frac{1}{2\pi i} \int_{-\infty}^{\infty} d\Omega \frac{e^{-i\Omega(t_i - t_j)}}{\Omega + i\epsilon}, \quad (29)$$

it is straightforward to derive the spectral integral representations in momentum space:

$$G_{R1}(\omega_1, \omega_2, \omega_3, \omega_4) = \oint a_1^+ [a_{12}^+(a_3^- + a_4^-) + a_{13}^+(a_2^- + a_4^-) + a_{14}^+(a_2^- + a_3^-)] \rho_{12}, \quad (30a)$$

$$G_{R2}(\omega_1, \omega_2, \omega_3, \omega_4) = \oint a_2^+ [a_{21}^+(a_3^- + a_4^-) + a_{23}^+(a_1^- + a_4^-) + a_{24}^+(a_1^- + a_3^-)] (-\rho_{12}), \quad (30b)$$

$$G_{R3}(\omega_1, \omega_2, \omega_3, \omega_4) = \oint a_3^+ [a_{31}^+(a_2^- + a_4^-) + a_{32}^+(a_1^- + a_4^-) + a_{34}^+(a_1^- + a_2^-)] \rho_{12}, \quad (30c)$$

$$G_{R4}(\omega_1, \omega_2, \omega_3, \omega_4) = \oint a_4^+ [a_{41}^+(a_2^- + a_3^-) + a_{42}^+(a_1^- + a_3^-) + a_{43}^+(a_1^- + a_2^-)] (-\rho_{12}), \quad (30d)$$

$$G_{rraa}(\omega_1, \omega_2, \omega_3, \omega_4) = \oint \left( a_1^+ [a_{12}^+(a_3^- + a_4^-) + a_{13}^+(a_2^- + a_4^-) + a_{14}^+(a_2^- + a_3^-)] \right. \\ \left. + a_2^+ [a_{21}^+(a_3^- + a_4^-) + a_{23}^+(a_1^- + a_4^-) + a_{24}^+(a_1^- + a_3^-)] \right) \rho_3, \quad (30e)$$

$$G_{rara}(\omega_1, \omega_2, \omega_3, \omega_4) = \oint \left( a_1^+ [a_{12}^+(a_3^- + a_4^-) + a_{13}^+(a_2^- + a_4^-) + a_{14}^+(a_2^- + a_3^-)] \right. \\ \left. + a_3^+ [a_{31}^+(a_2^- + a_4^-) + a_{32}^+(a_1^- + a_4^-) + a_{34}^+(a_1^- + a_2^-)] \right) \rho_4 \quad (30f)$$

$$G_{raar}(\omega_1, \omega_2, \omega_3, \omega_4) = \oint \left( a_1^+ [a_{12}^+(a_3^- + a_4^-) + a_{13}^+(a_2^- + a_4^-) + a_{14}^+(a_2^- + a_3^-)] \right. \\ \left. + a_4^+ [a_{41}^+(a_2^- + a_3^-) + a_{42}^+(a_1^- + a_3^-) + a_{43}^+(a_1^- + a_2^-)] \right) \rho_5 \quad (30g)$$

where

$$\oint = \frac{i}{(2\pi)^3} \int d\Omega_1 d\Omega_2 d\Omega_3 \quad (31a)$$

$$a_i^\pm = \frac{1}{\omega_i - \Omega_i \pm i\epsilon} \quad (31b)$$

$$a_{ij}^\pm = \frac{1}{\omega_i + \omega_j - \Omega_j - \Omega_j \pm i\epsilon}; \quad i, j = 1, 2, 3, 4. \quad (31c)$$

The frequency arguments of the spectral functions under the integrals are  $\rho_i(\Omega_1, \Omega_2, \Omega_3, \Omega_4)$  with  $\Omega_1 + \Omega_2 + \Omega_3 + \Omega_4 = 0$ . The spatial momenta  $\mathbf{p}_1, \mathbf{p}_2, \mathbf{p}_3$ , and  $\mathbf{p}_4 = -(\mathbf{p}_1 + \mathbf{p}_2 + \mathbf{p}_3)$  are the same on both sides of these equations and have therefore been suppressed.

We have written the seven vertex functions (10) in terms of one complex spectral density ( $\rho_{12} \equiv \rho_1 + i\rho_2$ ) and three purely imaginary spectral densities ( $\rho_3, \rho_4, \rho_5$ ). This means that all sixteen 4-point functions can be expressed in terms of five real spectral densities:

$$\rho_1 = \text{Re} [n_B^{-1}(p_{20})G_{2122} + 2n_B^{-1}(p_{20} + p_{40})G_{2121} + n_B^{-1}(p_{40})G_{2221} - n_B^{-1}(p_{10})G_{1222} - n_B^{-1}(p_{30})G_{2212}], \quad (32a)$$

$$\rho_2 = -\text{Im} [n_F^{-1}(p_{20})G_{2122} + 2n_F^{-1}(p_{20} + p_{40})G_{2121} + n_F^{-1}(p_{40})G_{2221} - n_F^{-1}(p_{10})G_{1222} - n_F^{-1}(p_{30})G_{2212}], \quad (32b)$$

$$\bar{\rho}_3 = -i\rho_3 = 2 \text{Im} G_{rraa}, \quad (32c)$$

$$\bar{\rho}_4 = -i\rho_4 = 2 \text{Im} G_{rara}, \quad (32d)$$

$$\bar{\rho}_5 = -i\rho_5 = 2 \text{Im} G_{raar}, \quad (32e)$$

where we used the following relations in momentum space resulting from the KMS condition [21]:

$$G_{1211} = e^{\beta p_{20}} G_{2122}^*, \quad G_{1212} = e^{\beta(p_{20} + p_{40})} G_{2121}^*, \quad G_{1112} = e^{\beta p_{40}} G_{2221}^*, \quad (33a)$$

$$G_{2111} = e^{\beta p_{10}} G_{1222}^*, \quad G_{1121} = e^{\beta p_{30}} G_{2212}^*, \quad (33b)$$

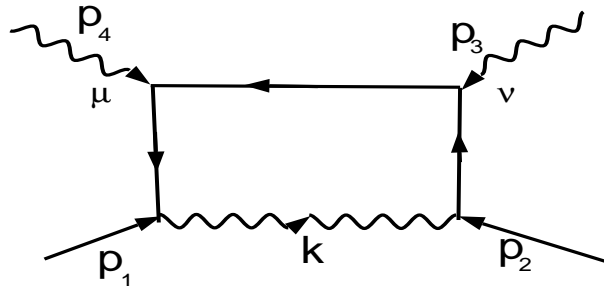
$$\tilde{G}_{rraa} = G_{rraa}^*, \quad \tilde{G}_{rara} = G_{rara}^*, \quad \tilde{G}_{raar} = G_{raar}^*. \quad (33c)$$

These results should be compared with the expressions derived in [15] in which the spectral representations for the four retarded functions  $G_{Ri}$ ,  $i = 1, 2, 3, 4$  were given in terms of three real spectral densities. A relation between these three spectral densities exists which can be employed to reduce the number of independent spectral functions to two; this is consistent with our result. Spectral representations for the mixed retarded-advanced 4-point functions have also been previously discussed: in [17], using a different definition of the mixed retarded-advanced 4-point functions, the spectral representation for one of these vertices was given in terms of six spectral densities.

We finally note that in deriving the spectral representations (30) no use was made of the KMS condition. In this form, (with the spectral densities defined by (16), (26) and (28)), Eqs. (30) remain valid out of thermal equilibrium.

#### IV. 4-POINT VERTEX FUNCTIONS IN QED IN THE HTL APPROXIMATION

In this section, we calculate the seven 4-point vertex functions (10) for QED in the HTL approximation. In the HTL approximation QED has two non-zero 4-point vertex functions, shown in Fig. [1] below:



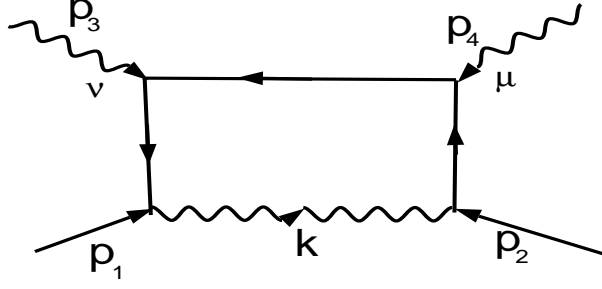


Fig. [1]: 4-point vertex in QED (a - upper graph) and its cross term (b - lower graph).

The other two 4-point vertex functions (four-photon vertex and four-fermion vertex) are zero in the HTL approximation [3]. We calculate the diagrams in Fig. [1] as follows: the real-time Green functions are written in the Keldysh formalism using (5) and (10). The photon propagator in the Feynman gauge is given by  $-ig_{\mu\nu}D(K)$  where  $D(K)$  is defined in (6). The fermion propagator is defined in (7). For the diagram in Fig. [1a] we obtain

$$G_{R1}^{\mu\nu(a)}(P_1, P_2, P_3, P_4) = \frac{1}{2} \int \frac{d^4 K}{(2\pi)^4} H^{\mu\nu}(K) [a_1 \bar{a}_2 \bar{a}_3 \bar{a}_4 + r_1 \bar{r}_2 \bar{r}_3 \bar{r}_4 + f_1 \bar{a}_2 \bar{a}_3 \bar{a}_4 + r_1 \bar{f}_2 \bar{a}_3 \bar{a}_4 + r_1 \bar{r}_2 \bar{f}_3 \bar{a}_4 + r_1 \bar{r}_2 \bar{r}_3 \bar{f}_4], \quad (34a)$$

$$G_{R2}^{\mu\nu(a)}(P_1, P_2, P_3, P_4) = \frac{1}{2} \int \frac{d^4 K}{(2\pi)^4} H^{\mu\nu}(K) [a_1 \bar{a}_2 \bar{a}_3 \bar{a}_4 + r_1 \bar{r}_2 \bar{r}_3 \bar{r}_4 + f_1 \bar{r}_2 \bar{r}_3 \bar{r}_4 + a_1 \bar{f}_2 \bar{a}_3 \bar{a}_4 + a_1 \bar{r}_2 \bar{f}_3 \bar{a}_4 + a_1 \bar{r}_2 \bar{r}_3 \bar{f}_4], \quad (34b)$$

$$G_{R3}^{\mu\nu(a)}(P_1, P_2, P_3, P_4) = \frac{1}{2} \int \frac{d^4 K}{(2\pi)^4} H^{\mu\nu}(K) [a_1 \bar{a}_2 \bar{a}_3 \bar{a}_4 + r_1 \bar{r}_2 \bar{r}_3 \bar{r}_4 + f_1 \bar{a}_2 \bar{r}_3 \bar{r}_4 + r_1 \bar{f}_2 \bar{r}_3 \bar{r}_4 + a_1 \bar{a}_2 \bar{f}_3 \bar{a}_4 + a_1 \bar{a}_2 \bar{r}_3 \bar{f}_4], \quad (34c)$$

$$G_{R4}^{\mu\nu(a)}(P_1, P_2, P_3, P_4) = \frac{1}{2} \int \frac{d^4 K}{(2\pi)^4} H^{\mu\nu}(K) [a_1 \bar{a}_2 \bar{a}_3 \bar{a}_4 + r_1 \bar{r}_2 \bar{r}_3 \bar{r}_4 + f_1 \bar{a}_2 \bar{a}_3 \bar{r}_4 + r_1 \bar{f}_2 \bar{a}_3 \bar{r}_4 + r_1 \bar{r}_2 \bar{f}_3 \bar{r}_4 + a_1 \bar{a}_2 \bar{a}_3 \bar{f}_4], \quad (34d)$$

$$G_{rara}^{\mu\nu(a)}(P_1, P_2, P_3, P_4) = \frac{1}{2} \int \frac{d^4 K}{(2\pi)^4} H^{\mu\nu}(K) [a_1 \bar{a}_2 \bar{a}_3 \bar{a}_4 + r_1 \bar{r}_2 \bar{r}_3 \bar{r}_4 + f_1 \bar{a}_2 \bar{f}_3 \bar{a}_4 + r_1 \bar{a}_4 \bar{f}_2 \bar{f}_3 + r_1 \bar{r}_2 \bar{a}_3 \bar{a}_4 + f_1 \bar{a}_2 \bar{r}_3 \bar{f}_4 + r_1 \bar{r}_3 \bar{f}_2 \bar{f}_4 + a_1 \bar{a}_2 \bar{r}_3 \bar{r}_4], \quad (34e)$$

$$G_{rraa}^{\mu\nu(a)}(P_1, P_2, P_3, P_4) = \frac{1}{2} \int \frac{d^4 K}{(2\pi)^4} H^{\mu\nu}(K) [a_1 \bar{a}_2 \bar{a}_3 \bar{a}_4 + r_1 \bar{r}_2 \bar{r}_3 \bar{r}_4 + r_1 \bar{a}_2 \bar{a}_3 \bar{a}_4 + a_1 \bar{r}_2 \bar{r}_3 \bar{r}_4 + f_1 \bar{f}_2 \bar{a}_3 \bar{a}_4 + f_1 \bar{f}_3 \bar{r}_2 \bar{a}_4 + f_1 \bar{f}_4 \bar{r}_2 \bar{r}_3], \quad (34f)$$

$$G_{raar}^{\mu\nu(a)}(P_1, P_2, P_3, P_4) = \frac{1}{2} \int \frac{d^4 K}{(2\pi)^4} H^{\mu\nu}(K) [a_1 \bar{a}_2 \bar{a}_3 \bar{a}_4 + r_1 \bar{r}_2 \bar{r}_3 \bar{r}_4 + a_1 \bar{a}_2 \bar{a}_3 \bar{r}_4 + r_1 \bar{r}_2 \bar{r}_3 \bar{a}_4 + f_1 \bar{f}_4 \bar{a}_2 \bar{a}_3 + \bar{f}_2 \bar{f}_4 r_1 \bar{a}_3 + \bar{f}_3 \bar{f}_4 r_1 \bar{r}_2], \quad (34g)$$

where

$$H_{\mu\nu}(K) = e^4 \gamma_\alpha (\not{K} - \not{P}_1 + m) \gamma_\mu (\not{P}_2 + \not{P}_3 + \not{K} + m) \gamma_\nu (\not{P}_2 + \not{K} + m) \gamma_\alpha \quad (35)$$

and we used the notation  $a_1 = D_A(K)$ ,  $r_1 = D_R(K)$ ,  $f_1 = D_F(K)$  for photon propagators and  $\bar{a}_j = \bar{D}_A(K_j)$ ,  $\bar{r}_j = \bar{D}_R(K_j)$ ,  $\bar{f}_j = \bar{D}_F(K_j)$  [ $j = 2, 3, 4$  and  $K_2 = P_2 + K$ ,  $K_3 = P_2 + P_3 + K$ ,  $K_4 = K - P_1$ ] for electron propagators. Note that the first two terms in each equation of (34) vanish by contour integration since all poles are located on the same side of the real axis.

Before doing any momentum integrations, we can see immediately from (34) that the one-loop retarded functions ( $G_{Ri}$ ,  $i = 1, 2, 3, 4$ ) are linear in the distribution functions, since they are linear in the symmetric propagators  $f_i$  and/or  $\bar{f}_i$ . Terms with higher powers of the distribution functions are explicitly cancelled in the Keldysh formalism. This type of cancellation also occurs for the 2- and 3-point retarded-advanced functions [27]. In contrast, the mixed

retarded-advanced functions are bilinear in the distribution functions. One of the advantages of the Keldysh formalism is that it allows us to immediately identify the leading order temperature dependence.

In the HTL approximation, the external momenta are soft (of order  $eT$  with  $e \ll 1$ ) and the loop momenta are hard (of order  $T$ ) [4,5]. In this approximation, we can neglect the external momenta and the bare electron mass  $m$  relative to the loop momenta. For  $H_{\mu\nu}(K)$  one then obtains

$$H_{\mu\nu}(K) \approx 8e^4 K_\mu K_\nu \bar{K}. \quad (36)$$

We first consider  $G_{R1}^a$ . Fig. [1a] gives

$$\begin{aligned} G_{R1}^{\mu\nu(a)}(P_1, P_2, P_3, P_4) &= \frac{1}{2} \int \frac{d^4 K}{(2\pi)^4} H^{\mu\nu}(K) [f_1 \bar{a}_2 \bar{a}_3 \bar{a}_4 + r_1 \bar{f}_2 \bar{a}_3 \bar{a}_4 + r_1 \bar{r}_2 \bar{f}_3 \bar{a}_4 + r_1 \bar{r}_2 \bar{r}_3 \bar{f}_4] \\ &= I_1 + I_2 + I_3 + I_4. \end{aligned} \quad (37)$$

From (6), (7) we have

$$\begin{aligned} a_i(K) &= \bar{a}_i(K) = \frac{1}{K^2 - m_i^2 - i \text{sgn}(k_0) \epsilon}, \\ r_i(K) &= \bar{r}_i(K) = \frac{1}{K^2 - m_i^2 + i \text{sgn}(k_0) \epsilon}, \\ f_1(K) &= -2\pi i \delta(K^2) (1 + 2n_B(k)), \\ \bar{f}_i(K) &= -2\pi i \delta(K^2 - m_i^2) (1 - 2n_F(k)), \end{aligned} \quad (38)$$

where  $i=2, 3, 4$  and  $m_2=m_3=m_4=m$  which stands for the electron mass. We calculate the contribution from each of the terms in (37) in the HTL approximation:  $K \sim T \gg P_1, P_2, P_3, P_4, m$ . For the temperature-dependent contributions we obtain

$$I_1 = \frac{ie^4}{(2\pi)^3} \int dk k n_B(k) \int d\Omega V^\mu V^\nu \bar{V} \cdot b_{23}^- b_1^+ b_2^-, \quad (39a)$$

$$I_2 = \frac{ie^4}{(2\pi)^3} \int dk k n_F(k) \int d\Omega V^\mu V^\nu \bar{V} \cdot b_2^- b_3^- b_{12}^+, \quad (39b)$$

$$I_3 = \frac{ie^4}{(2\pi)^3} \int dk k n_F(k) \int d\Omega V^\mu V^\nu \bar{V} \cdot b_3^- b_4^- b_{23}^-, \quad (39c)$$

$$I_4 = -\frac{ie^4}{(2\pi)^3} \int dk k n_F(k) \int d\Omega V^\mu V^\nu \bar{V} \cdot b_1^+ b_4^- b_{12}^+, \quad (39d)$$

where

$$b_i^\pm = \frac{1}{P_i \cdot V \pm i\epsilon}, \quad (40a)$$

$$b_{ij}^\pm = \frac{1}{(P_i + P_j) \cdot V \pm i\epsilon}, \quad i, j = 1, 2, 3, 4, \quad (40b)$$

and  $V = (1, \mathbf{V})$  with  $\mathbf{V} = \mathbf{k}/k$  a light-like unit vector, and  $\int d\Omega$  denotes integration over the orientation of  $\mathbf{V}$ .

By interchanging  $P_3$  and  $P_4$  we obtain the contribution from Fig. [1b] to  $G_{R1}$ :

$$G_{R1}^{\mu\nu(b)} = J_1 + J_2 + J_3 + J_4, \quad (41)$$

with

$$J_1 = \frac{ie^4}{(2\pi)^3} \int dk k n_B(k) \int d\Omega V^\mu V^\nu \bar{V} \cdot b_1^+ b_2^- b_{24}^-, \quad (42a)$$

$$J_2 = \frac{ie^4}{(2\pi)^3} \int dk k n_F(k) \int d\Omega V^\mu V^\nu \bar{V} \cdot b_2^- b_4^- b_{12}^+, \quad (42b)$$

$$J_3 = \frac{ie^4}{(2\pi)^3} \int dk k n_F(k) \int d\Omega V^\mu V^\nu \bar{V} \cdot b_3^- b_4^- b_{24}^-, \quad (42c)$$

$$J_4 = -\frac{ie^4}{(2\pi)^3} \int dk k n_F(k) \int d\Omega V^\mu V^\nu \bar{V} \cdot b_1^+ b_4^- b_{12}^+. \quad (42d)$$

Combining (39) and (42), the total contribution to  $G_{R1}^{\mu\nu}$  from Fig. [1] reads

$$G_{R1}^{\mu\nu}(P_1, P_2, P_3, P_4) = G_{R1}^{\mu\nu(a)} + G_{R1}^{\mu\nu(b)} = \frac{ie^2 m_\beta^2}{4\pi} \int d\Omega V^\mu V^\nu \bar{\Psi} \cdot b_{23}^- b_{24}^- (b_1^+ - b_2^-) \quad (43)$$

where

$$m_\beta^2 = \frac{e^2}{2\pi^2} \int dk k (n_B(k) + n_F(k)) = \frac{e^2 T^2}{8} \quad (44)$$

is the usual expression for the square of the dynamically generated thermal electron mass.

Proceeding similarly, we can calculate the other three retarded 4-point functions in finite temperature QED in the HTL approximation. The final results, including both diagrams in Fig. [1], are

$$G_{R2}^{\mu\nu}(P_1, P_2, P_3, P_4) = \frac{ie^2 m_\beta^2}{4\pi} \int d\Omega V^\mu V^\nu \bar{\Psi} b_{23}^+ b_{24}^+ (b_1^- - b_2^+), \quad (45a)$$

$$G_{R3}^{\mu\nu}(P_1, P_2, P_3, P_4) = \frac{ie^2 m_\beta^2}{4\pi} \int d\Omega V^\mu V^\nu \bar{\Psi} b_{23}^+ b_{24}^+ (b_1^- - b_2^-), \quad (45b)$$

$$G_{R4}^{\mu\nu}(P_1, P_2, P_3, P_4) = \frac{ie^2 m_\beta^2}{4\pi} \int d\Omega V^\mu V^\nu \bar{\Psi} b_{23}^- b_{24}^- (b_1^- - b_2^-). \quad (45c)$$

Our results agree with those obtained in the ITF [18]; to leading order, all of the retarded 4-point functions are proportional to  $T^2$ .

Next we consider the mixed retarded-advanced 4-point functions. We begin with  $G_{rara}^{\mu\nu}$ . The leading order temperature-dependent piece from Fig. [1a] is

$$\begin{aligned} G_{rara}^{\mu\nu(a)}(P_1, P_2, P_3, P_4) &= \frac{1}{2} \int \frac{d^4 K}{(2\pi)^4} H^{\mu\nu}(K) [f_1 \bar{a}_2 \bar{f}_3 \bar{a}_4 + r_1 \bar{f}_2 \bar{f}_3 \bar{a}_4 + f_1 \bar{a}_2 \bar{r}_3 \bar{f}_4 + r_1 \bar{r}_3 \bar{f}_2 \bar{f}_4] \\ &= T_1 + T_2 + T_3 + T_4, \end{aligned} \quad (46)$$

where the functions  $T_i$ ;  $i = \{1, 2, 3, 4\}$  represent the contributions of the four terms respectively. Inserting the propagators (38) and using the HTL approximation we find

$$T_1 = \frac{e^4}{(2\pi)^3} c_\beta \int d\Omega V^\mu V^\nu \bar{\Psi} b_1^+ b_2^- (b_{23}^- - b_{23}^+), \quad (47a)$$

$$T_2 = \frac{e^4}{(2\pi)^3} d_\beta \int d\Omega V^\mu V^\nu \bar{\Psi} b_{12}^+ b_2^- (b_3^- - b_3^+), \quad (47b)$$

$$T_3 = \frac{e^4}{(2\pi)^3} c_\beta \int d\Omega V^\mu V^\nu \bar{\Psi} b_2^- b_{23}^+ (b_1^+ - b_1^-), \quad (47c)$$

$$T_4 = \frac{e^4}{(2\pi)^3} d_\beta \int d\Omega V^\mu V^\nu \bar{\Psi} b_3^+ b_2^- (b_{12}^+ - b_{12}^-), \quad (47d)$$

where

$$\begin{aligned} c_\beta &= \int dk k [n_B(k)(1 - n_F(k)) - n_F(k)(1 + n_B(k))], \\ d_\beta &= -2 \int dk k n_F(k)(1 - n_F(k)). \end{aligned} \quad (48)$$

Inserting the standard forms for the Bose-Einstein and Fermi-Dirac distributions we obtain in thermal equilibrium

$$c_\beta = 0, \quad d_\beta = -(2 \ln 2) T^2. \quad (49)$$

The contribution from Fig. [1b] to  $G_{rara}^{\mu\nu}$  is

$$G_{rara}^{\mu\nu(b)} = S_1 + S_2 + S_3 + S_4 \quad (50)$$

with

$$S_1 = \frac{e^4}{(2\pi)^3} c_\beta \int d\Omega V^\mu V^\nu \mathcal{V} b_1^+ b_2^- (b_{24}^- - b_{24}^+), \quad (51a)$$

$$S_2 = \frac{e^4}{(2\pi)^3} d_\beta \int d\Omega V^\mu V^\nu \mathcal{V} b_{12}^+ b_2^- (b_4^- - b_4^+), \quad (51b)$$

$$S_3 = \frac{e^4}{(2\pi)^3} c_\beta \int d\Omega V^\mu V^\nu \mathcal{V} b_2^- b_{24}^+ (b_1^+ - b_1^-), \quad (51c)$$

$$S_4 = \frac{e^4}{(2\pi)^3} d_\beta \int d\Omega V^\mu V^\nu \mathcal{V} b_4^+ b_2^- (b_{12}^+ - b_{12}^-). \quad (51d)$$

Adding (47) and (51) we obtain

$$G_{rara}^{\mu\nu} = \frac{e^4}{(2\pi)^3} \int d\Omega V^\mu V^\nu \mathcal{V} \left[ d_\beta b_2^- (b_{12}^+ (b_3^- + b_4^-) - b_{12}^- (b_3^+ + b_4^+)) + c_\beta b_2^- (b_1^+ (b_{23}^- + b_{24}^-) - b_1^- (b_{24}^+ + b_{23}^+)) \right]. \quad (52)$$

In spite of (49) we keep the terms  $\sim c_\beta$  because we will discuss the extension of these results to non-equilibrium situations in Sec. VII.

The other two mixed retarded-advanced 4-point functions are similarly calculated:

$$\begin{aligned} G_{raar}^{\mu\nu} &= \frac{e^4}{(2\pi)^3} \int d\Omega V^\mu V^\nu \mathcal{V} \left[ d_\beta b_1^+ (b_{12}^+ (b_3^- + b_4^-) - b_{12}^- (b_3^+ + b_4^+)) + c_\beta b_2^- (b_1^+ (b_{23}^- + b_{24}^-) - b_1^- (b_{24}^+ + b_{23}^+)) \right], \\ G_{rraa}^{\mu\nu} &= \frac{e^4}{(2\pi)^3} \int d\Omega V^\mu V^\nu \mathcal{V} \left[ c_\beta (b_2^- b_1^+ (b_{23}^- + b_{24}^-) - b_2^+ b_1^- (b_{24}^+ + b_{23}^+)) \right]. \end{aligned} \quad (53)$$

The last function vanishes in equilibrium since  $c_\beta = 0$ . The other mixed retarded-advanced 4-point functions are again proportional to  $T^2$ . Furthermore, since  $V^2=0$ , all seven 4-point functions are traceless ( $G_\mu^\mu = 0$ ) in the HTL approximation.

## V. 4-POINT SPECTRAL FUNCTIONS IN HOT QED IN THE HTL APPROXIMATION

From (43), (45), (52) and (53) one obtains the following spectral representations for the 4-point retarded-advanced functions in the HTL approximation:

$$G_{R1}^{\mu\nu}(\omega_1, \omega_2, \omega_3, \omega_4) = \frac{i}{(2\pi)^3} \int d\Omega_1 d\Omega_2 d\Omega_3 d\Omega_4 \delta(\Omega_1 + \Omega_2 + \Omega_3 + \Omega_4) \rho_{\text{HTL}}^{\mu\nu}(\Omega_1, \Omega_2, \Omega_3, \Omega_4) a_{23}^- a_{24}^+ (a_1^+ - a_2^-), \quad (54a)$$

$$G_{R2}^{\mu\nu}(\omega_1, \omega_2, \omega_3, \omega_4) = \frac{i}{(2\pi)^3} \int d\Omega_1 d\Omega_2 d\Omega_3 d\Omega_4 \delta(\Omega_1 + \Omega_2 + \Omega_3 + \Omega_4) \rho_{\text{HTL}}^{\mu\nu}(\Omega_1, \Omega_2, \Omega_3, \Omega_4) a_{23}^+ a_{24}^+ (a_1^- - a_2^+), \quad (54b)$$

$$G_{R3}^{\mu\nu}(\omega_1, \omega_2, \omega_3, \omega_4) = \frac{i}{(2\pi)^3} \int d\Omega_1 d\Omega_2 d\Omega_3 d\Omega_4 \delta(\Omega_1 + \Omega_2 + \Omega_3 + \Omega_4) \rho_{\text{HTL}}^{\mu\nu}(\Omega_1, \Omega_2, \Omega_3, \Omega_4) a_{23}^+ a_{24}^+ (a_1^- - a_2^-), \quad (54c)$$

$$G_{R4}^{\mu\nu}(\omega_1, \omega_2, \omega_3, \omega_4) = \frac{i}{(2\pi)^3} \int d\Omega_1 d\Omega_2 d\Omega_3 d\Omega_4 \delta(\Omega_1 + \Omega_2 + \Omega_3 + \Omega_4) \rho_{\text{HTL}}^{\mu\nu}(\Omega_1, \Omega_2, \Omega_3, \Omega_4) a_{23}^- a_{24}^- (a_1^- - a_2^-), \quad (54d)$$

$$\begin{aligned} G_{rara}^{\mu\nu}(\omega_1, \omega_2, \omega_3, \omega_4) &= \frac{i}{(2\pi)^3} \int d\Omega_1 d\Omega_2 d\Omega_3 d\Omega_4 \delta(\Omega_1 + \Omega_2 + \Omega_3 + \Omega_4) \rho_{\text{HTL}}^{\mu\nu}(\Omega_1, \Omega_2, \Omega_3, \Omega_4) \\ &\quad \cdot \left[ \alpha_1 a_2^- (a_{12}^+ (a_3^- + a_4^-) - a_{12}^- (a_3^+ + a_4^+)) + \alpha_2 (a_2^- a_1^+ (a_{23}^- + a_{24}^-) - a_2^- a_1^- (a_{24}^+ + a_{23}^+)) \right], \end{aligned} \quad (54e)$$

$$\begin{aligned} G_{raar}^{\mu\nu}(\omega_1, \omega_2, \omega_3, \omega_4) &= \frac{i}{(2\pi)^3} \int d\Omega_1 d\Omega_2 d\Omega_3 d\Omega_4 \delta(\Omega_1 + \Omega_2 + \Omega_3 + \Omega_4) \rho_{\text{HTL}}^{\mu\nu}(\Omega_1, \Omega_2, \Omega_3, \Omega_4) \\ &\quad \cdot \left[ \alpha_1 a_1^+ (a_{12}^+ (a_3^- + a_4^-) - a_{12}^- (a_3^+ + a_4^+)) + \alpha_2 a_2^- a_1^+ (a_{23}^- + a_{24}^-) - a_2^- a_1^- (a_{24}^+ + a_{23}^+) \right], \end{aligned} \quad (54f)$$

$$\begin{aligned} G_{rraa}^{\mu\nu}(\omega_1, \omega_2, \omega_3, \omega_4) &= \frac{i}{(2\pi)^3} \int d\Omega_1 d\Omega_2 d\Omega_3 d\Omega_4 \delta(\Omega_1 + \Omega_2 + \Omega_3 + \Omega_4) \rho_{\text{HTL}}^{\mu\nu}(\Omega_1, \Omega_2, \Omega_3, \Omega_4) \\ &\quad \cdot \left[ \alpha_2 (a_2^- a_1^+ (a_{23}^- + a_{24}^-) - a_2^+ a_1^- (a_{24}^+ + a_{23}^+)) \right], \end{aligned} \quad (54g)$$

where

$$\rho_{\text{HTL}}^{\mu\nu}(\Omega_1, \Omega_2, \Omega_3, \Omega_4) = 2\pi^2 e^2 m_\beta^2 \int d\Omega V^\mu V^\nu \mathcal{V} \delta(\tilde{P}_1 \cdot V) \delta(\tilde{P}_2 \cdot V) \delta(\tilde{P}_3 \cdot V) \quad (55)$$

(with  $\tilde{P}_i^0 \equiv \Omega_i$ ,  $\tilde{\mathbf{P}}_i = \mathbf{P}_i$ ;  $i=\{1, 2, 3\}$  on the r.h.s.) and

$$\alpha_1 = \frac{d_\beta e^4}{2i\pi^2 e^2 m_\beta^2}; \quad \alpha_2 = \frac{c_\beta e^4}{2i\pi^2 e^2 m_\beta^2}. \quad (56)$$

These equations also hold in the non-equilibrium situations studied in Sec. VII. In equilibrium we use (49) to obtain

$$\alpha_1 = i \frac{8 \ln 2}{\pi^2}; \quad \alpha_2 = 0 \quad (57)$$

Note that the frequencies  $\Omega_i$  should not be confused with the angular factor  $\Omega$ . From  $V^2=0$  it follows that

$$(\rho_{\text{HTL}})^\mu_\mu = 0. \quad (58)$$

In contrast to the general spectral representations (30) of the 4-point functions given in Sec. III, in the HTL approximation the spectral representations (54) involve only a single, real-valued spectral density  $\rho_{\text{HTL}}^{\mu\nu}$ . This agrees with the result of Taylor [18] who showed for QCD in the ITF that in the HTL approximation all spectral densities degenerate to a single function. Clearly, the spectral density (55) is symmetric in the Lorentz indices and under interchange of the external momenta. Using the  $\delta$ -functions in (55) it is also easy to show that  $\rho_{\text{HTL}}^{\mu\nu}$  is transverse with respect to all external momenta:

$$P_\mu^i \rho_{\text{HTL}}^{\mu\nu} = 0, \quad i = 1, 2, 3, 4. \quad (59)$$

A previous RTF calculation of the 3-point spectral function in hot QED in the HTL approximation gave [26]

$$\rho_{\text{HTL}}^\mu(\Omega_1, \Omega_2, \Omega_3) = \frac{\pi e m_\beta^2}{2} \int d\Omega V^\mu \mathcal{V} \delta(\tilde{P}_1 \cdot V) \delta(\tilde{P}_2 \cdot V). \quad (60)$$

By comparing (55) with (59) we find the “sum rule”

$$\int d\Omega_3 \rho_{\text{HTL}}^{\mu 0}(\Omega_1, \Omega_2, \Omega_3, -(\Omega_1 + \Omega_2 + \Omega_3)) = 4\pi e \rho_{\text{HTL}}^\mu(\Omega_1, \Omega_2, -(\Omega_1 + \Omega_2)). \quad (61)$$

This agrees with the ITF results in [18]. A similar sum rule exists between the 2- and 3-point spectral densities: the 2-point spectral density is given by

$$\rho_{\text{HTL}}(\Omega_1, -\Omega_1) = \frac{m_\beta^2}{2} \int d\Omega \mathcal{V} \delta(\tilde{P}_1 \cdot V), \quad (62)$$

and the temporal component of the 3-point spectral density  $\rho_{\text{HTL}}^\mu(\Omega_1, \Omega_2, -(\Omega_1 + \Omega_2))$  obeys the sum rule

$$\int d\Omega_2 \rho_{\text{HTL}}^0(\Omega_1, \Omega_2, -(\Omega_1 + \Omega_2)) = \pi e \rho_{\text{HTL}}(\Omega_1, -\Omega_1). \quad (63)$$

We believe that analogous sum rules exist for the higher order  $n$ -point functions.

## VI. WARD IDENTITIES BETWEEN 3- AND 4-POINT FUNCTIONS IN THE HTL APPROXIMATION

In this section, we verify the HTL Ward identities between the 3- and 4-point vertex functions in QED, without doing momentum integrations. We split propagators in the integral expressions (34) by using the identities [28]

$$\bar{D}_{R/A}(K_2) \bar{D}_{R/A}(K_3) = \frac{1}{K_3^2 - K_2^2} \left( \bar{D}_{R/A}(K_2) - \bar{D}_{R/A}(K_3) \right) \quad (64)$$

This trick allows us to rewrite (34) as

$$G_{R1}^{\mu\nu(a)} = e^4 \int \frac{d^4 K}{(2\pi)^4} \frac{4K^\mu K^\nu K}{2P_3 \cdot K} [f_1(\bar{a}_2 - \bar{a}_3)\bar{a}_4 + r_1\bar{f}_2\bar{a}_4 - r_1\bar{f}_3\bar{a}_4 + r_1(\bar{r}_2 - \bar{r}_3)\bar{f}_4], \quad (65a)$$

$$G_{R2}^{\mu\nu(a)} = e^4 \int \frac{d^4 K}{(2\pi)^4} \frac{4K^\mu K^\nu K}{2P_3 \cdot K} [f_1(\bar{r}_2 - \bar{r}_3)\bar{r}_4 + a_1\bar{f}_2\bar{a}_4 - a_1\bar{f}_3\bar{a}_4 + a_1(\bar{r}_2 - \bar{r}_3)\bar{f}_4], \quad (65b)$$

$$G_{R3}^{\mu\nu(a)} = e^4 \int \frac{d^4 K}{(2\pi)^4} \frac{4K^\mu K^\nu K}{2P_3 \cdot K} [f_1(\bar{a}_2 - \bar{r}_3)\bar{r}_4 + r_1\bar{f}_2\bar{r}_4 - a_1\bar{f}_3\bar{a}_4 + a_1(\bar{a}_2 - \bar{r}_3)\bar{f}_4], \quad (65c)$$

$$G_{R4}^{\mu\nu(a)} = e^4 \int \frac{d^4 K}{(2\pi)^4} \frac{4K^\mu K^\nu K}{2P_3 \cdot K} [f_1(\bar{a}_2 - \bar{a}_3)\bar{r}_4 + r_1\bar{f}_2\bar{r}_4 - r_1\bar{f}_3\bar{r}_4 + a_1(\bar{a}_2 - \bar{a}_3)\bar{f}_4], \quad (65d)$$

$$G_{rara}^{\mu\nu(a)} = e^4 \int \frac{d^4 K}{(2\pi)^4} \frac{4K^\mu K^\nu K}{2P_3 \cdot K} [-f_1\bar{f}_3\bar{a}_4 + r_1(\bar{r}_2 - \bar{a}_3)\bar{a}_4 + f_1(\bar{a}_2 - \bar{r}_3)\bar{f}_4 + r_1\bar{f}_2\bar{f}_4 + a_1(\bar{a}_2 - \bar{r}_3)\bar{r}_4], \quad (65e)$$

$$G_{rraa}^{\mu\nu(a)} = e^4 \int \frac{d^4 K}{(2\pi)^4} \frac{4K^\mu K^\nu K}{2P_3 \cdot K} [r_1(\bar{a}_2 - \bar{a}_3)\bar{a}_4 + a_1(\bar{r}_2 - \bar{r}_3)\bar{r}_4 + f_1\bar{f}_2\bar{a}_4 - f_1\bar{f}_3\bar{a}_4 + f_1\bar{f}_4(\bar{r}_2 - \bar{r}_3)], \quad (65f)$$

$$G_{raar}^{\mu\nu(a)} = e^4 \int \frac{d^4 K}{(2\pi)^4} \frac{4K^\mu K^\nu K}{2P_3 \cdot K} [a_1(\bar{a}_2 - \bar{a}_3)\bar{r}_4 + r_1(\bar{r}_2 - \bar{r}_3)\bar{a}_4 + f_1\bar{f}_4(\bar{a}_2 - \bar{a}_3) + \bar{f}_2\bar{f}_4r_1 - \bar{f}_3\bar{f}_4r_1], \quad (65g)$$

where we have used the HTL approximation to write  $K_3^2 - K_2^2 = 2K \cdot P_3 + P_3^2 \approx 2K \cdot P_3$ .

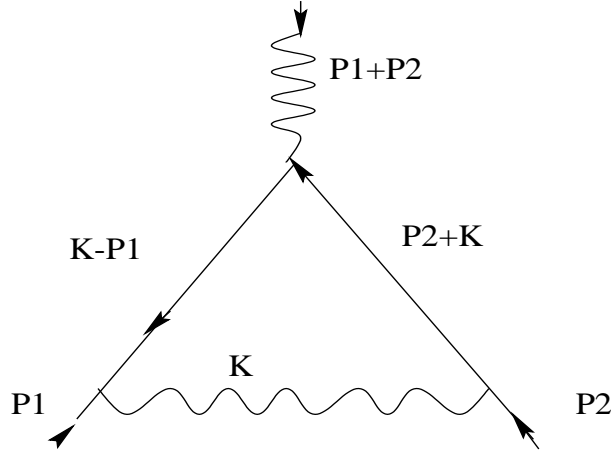


Fig. [2]: 3-point vertex in QED

The integral expressions for the 3-point vertex functions in QED are obtained from Fig. [2]. In the Feynman gauge we have

$$G_R^\mu(P_1, P_2, P_3+P_4) = e^3 \int \frac{d^4 K}{(2\pi)^4} (2K^\mu K) [a_1\bar{a}_2\bar{a}_4 + r_1\bar{r}_2\bar{r}_4 + f_1\bar{r}_2\bar{r}_4 + a_1\bar{f}_2\bar{a}_4 + a_1\bar{r}_2\bar{f}_4], \quad (66a)$$

$$G_{Ri}^\mu(P_1, P_2, P_3+P_4) = e^3 \int \frac{d^4 K}{(2\pi)^4} (2K^\mu K) [a_1\bar{a}_2\bar{a}_4 + r_1\bar{r}_2\bar{r}_4 + f_1\bar{a}_2\bar{a}_4 + r_1\bar{f}_2\bar{a}_4 + r_1\bar{r}_2\bar{f}_4], \quad (66b)$$

$$G_{Ro}^\mu(P_1, P_2, P_3+P_4) = e^3 \int \frac{d^4 K}{(2\pi)^4} (2K^\mu K) [a_1\bar{a}_2\bar{a}_4 + r_1\bar{r}_2\bar{r}_4 + f_1\bar{a}_2\bar{r}_4 + r_1\bar{f}_2\bar{r}_4 + a_1\bar{a}_2\bar{f}_4], \quad (66c)$$

$$G_F^\mu(P_1, P_2, P_3+P_4) = e^3 \int \frac{d^4 K}{(2\pi)^4} (2K^\mu K) [a_1\bar{a}_2\bar{r}_4 + r_1\bar{r}_2\bar{a}_4 + r_1\bar{f}_2\bar{f}_4 + f_1\bar{a}_2\bar{f}_4], \quad (66d)$$

$$G_{Fi}^\mu(P_1, P_2, P_3+P_4) = e^3 \int \frac{d^4 K}{(2\pi)^4} (2K^\mu K) [a_1\bar{r}_2\bar{a}_4 + r_1\bar{a}_2\bar{r}_4 + a_1\bar{f}_2\bar{f}_4 + f_1\bar{f}_2\bar{r}_4], \quad (66e)$$

$$G_{Fo}^\mu(P_1, P_2, P_3+P_4) = e^3 \int \frac{d^4 K}{(2\pi)^4} (2K^\mu K) [r_1\bar{a}_2\bar{a}_4 + a_1\bar{r}_2\bar{r}_4 + f_1\bar{f}_2\bar{a}_4 + f_1\bar{r}_2\bar{f}_4], \quad (66f)$$

where for later convenience we have chosen to write on the l.h.s.  $-(P_1+P_2) = P_3+P_4$ . Comparing (65) and (66) we obtain the following Ward identities between the vertices shown in Fig. [1a] and Fig. [2]:

$$P_{3\mu}G_{R1}^{\mu\nu(a)}(P_1, P_2, P_3, P_4) = e \left( G_{Ri}^\nu(P_1, P_2, P_3+P_4) - G_{Ri}^\nu(P_1, P_2+P_3, P_4) \right), \quad (67a)$$

$$P_{3\mu}G_{R2}^{\mu\nu(a)}(P_1, P_2, P_3, P_4) = e \left( G_R^\nu(P_1, P_2, P_3+P_4) - G_R^\nu(P_1, P_2+P_3, P_4) \right), \quad (67b)$$

$$P_{3\mu}G_{R3}^{\mu\nu(a)}(P_1, P_2, P_3, P_4) = e \left( G_{Ro}^\nu(P_1, P_2, P_3+P_4) - G_R^\nu(P_1, P_2+P_3, P_4) \right), \quad (67c)$$

$$P_{3\mu}G_{R4}^{\mu\nu(a)}(P_1, P_2, P_3, P_4) = e \left( G_{Ro}^\nu(P_1, P_2, P_3+P_4) - G_{Ro}^\nu(P_1, P_2+P_3, P_4) \right), \quad (67d)$$

$$P_{3\mu}G_{rara}^{\mu\nu(a)}(P_1, P_2, P_3, P_4) = e \left( G_F^\nu(P_1, P_2, P_3+P_4) - G_{Fo}^\nu(P_1, P_2+P_3, P_4) \right), \quad (67e)$$

$$P_{3\mu}G_{raar}^{\mu\nu(a)}(P_1, P_2, P_3, P_4) = e \left( G_F^\nu(P_1, P_2, P_3+P_4) - G_F^\nu(P_1, P_2+P_3, P_4) \right), \quad (67f)$$

$$P_{3\mu}G_{rraa}^{\mu\nu(a)}(P_1, P_2, P_3, P_4) = e \left( G_{Fo}^\nu(P_1, P_2, P_3+P_4) - G_{Fo}^\nu(P_1, P_2+P_3, P_4) \right). \quad (67g)$$

Similarly one can obtain the Ward identities satisfied by the diagrams in Fig. [1b] and Fig. [2]:

$$P_{3\mu}G_{R1}^{\mu\nu(b)}(P_1, P_2, P_3, P_4) = e \left( G_{Ri}^\nu(P_1+P_3, P_2, P_4) - G_{Ri}^\nu(P_1, P_2, P_3+P_4) \right), \quad (68a)$$

$$P_{3\mu}G_{R2}^{\mu\nu(b)}(P_1, P_2, P_3, P_4) = e \left( G_R^\nu(P_1+P_3, P_2, P_4) - G_R^\nu(P_1, P_2, P_3+P_4) \right), \quad (68b)$$

$$P_{3\mu}G_{R3}^{\mu\nu(b)}(P_1, P_2, P_3, P_4) = e \left( G_{Ro}^\nu(P_1+P_3, P_2, P_4) - G_{Ro}^\nu(P_1, P_2, P_3+P_4) \right), \quad (68c)$$

$$P_{3\mu}G_{R4}^{\mu\nu(b)}(P_1, P_2, P_3, P_4) = e \left( G_{Ri}^\nu(P_1+P_3, P_2, P_4) - G_{Ro}^\nu(P_1, P_2, P_3+P_4) \right), \quad (68d)$$

$$P_{3\mu}G_{rara}^{\mu\nu(b)}(P_1, P_2, P_3, P_4) = e \left( G_F^\nu(P_1+P_3, P_2, P_4) - G_F^\nu(P_1, P_2, P_3+P_4) \right), \quad (68e)$$

$$P_{3\mu}G_{raar}^{\mu\nu(b)}(P_1, P_2, P_3, P_4) = -e G_F^\nu(P_1, P_2, P_3+P_4), \quad (68f)$$

$$P_{3\mu}G_{rraa}^{\mu\nu(b)}(P_1, P_2, P_3, P_4) = e \left( G_{Fo}^\nu(P_1+P_3, P_2, P_4) - G_{Fo}^\nu(P_1, P_2, P_3+P_4) \right). \quad (68g)$$

By combining (67) and (68) one obtains the following HTL Ward identities between the 3- and 4-point vertex functions in QED in the RTF:

$$P_{3\mu}G_{R1}^{\mu\nu}(P_1, P_2, P_3, P_4) = e \left( G_{Ri}^\nu(P_1+P_3, P_2, P_4) - G_{Ri}^\nu(P_1, P_2+P_3, P_4) \right), \quad (69a)$$

$$P_{3\mu}G_{R2}^{\mu\nu}(P_1, P_2, P_3, P_4) = e \left( G_R^\nu(P_1+P_3, P_2, P_4) - G_R^\nu(P_1, P_2+P_3, P_4) \right), \quad (69b)$$

$$P_{3\mu}G_{R3}^{\mu\nu}(P_1, P_2, P_3, P_4) = e \left( G_R^\nu(P_1+P_3, P_2, P_4) - G_{Ro}^\nu(P_1, P_2+P_3, P_4) \right), \quad (69c)$$

$$P_{3\mu}G_{R4}^{\mu\nu}(P_1, P_2, P_3, P_4) = e \left( G_{Ro}^\nu(P_1+P_3, P_2, P_4) - G_{Ri}^\nu(P_1, P_2+P_3, P_4) \right), \quad (69d)$$

$$P_{3\mu}G_{rara}^{\mu\nu}(P_1, P_2, P_3, P_4) = e \left( G_F^\nu(P_1+P_3, P_2, P_4) - G_{Fo}^\nu(P_1, P_2+P_3, P_4) \right), \quad (69e)$$

$$P_{3\mu}G_{raar}^{\mu\nu}(P_1, P_2, P_3, P_4) = -e G_F^\nu(P_1, P_2+P_3, P_4), \quad (69f)$$

$$P_{3\mu}G_{rraa}^{\mu\nu}(P_1, P_2, P_3, P_4) = e \left( G_{Fo}^\nu(P_1+P_3, P_2, P_4) - G_{Fo}^\nu(P_1, P_2+P_3, P_4) \right). \quad (69g)$$

Notice that in equilibrium the last equation gives simply  $0 = 0$  (see (49) and (53)). These results are structurally similar to the zero temperature Ward identity [29] and to the Ward identities between the retarded 3- and 4-point HTL vertices in QCD obtained within the imaginary time formalism [8] or from kinetic theory [10].

## VII. EXTENSION TO NON-EQUILIBRIUM SITUATIONS

The HTL method has been widely used in qualitative studies of the QGP and in other explicit calculations at finite temperature [5]. This powerful method was derived within the ITF for equilibrium field theory, and this is where its range of applicability can be clearly defined [4,5,8]: HTL resummation is required and applicable for the study of soft processes in a weakly interacting plasma, with momentum scale  $p \sim gT \ll T$  ( $g \ll 1$ ) much below the typical thermal or “hard” momenta in the medium. Realistic physical systems, on the other hand, are frequently out of equilibrium, which means that calculations must be carried out in the RTF. As long as the local momentum distribution  $f(x, p)$

doesn't deviate too strongly from a thermal one, and can still be roughly characterized by a parameter  $T$  which gives the scale for the typical momenta at point  $x$ , a similar "hard loop" (HL) resummation scheme should be applicable for the study of the dynamics of soft modes ( $p \sim gT \ll T$ ) in a weakly interacting ( $g \ll 1$ ) non-equilibrium system [28]. This approach is expected to be reliable for equilibration processes requiring momentum exchanges which happen slowly, on a time scale  $\tau \sim (g^2 T)^{-1} \gg 1/p^0$ . This reasoning does not apply to arbitrary non-equilibrium situations, but only to plasma states which are sufficiently close to global thermal equilibrium; on the other hand, deviations from chemical equilibrium can be arbitrarily strong without invalidating the scheme.

In this section we discuss the generalization of our results to this particular type of non-equilibrium scenarios. Since we have used the Keldysh or closed time path contour, the procedure is straightforward. Equations (1) and (2) can be used in non-equilibrium situations by replacing the  $x$ -independent equilibrium Bose-Einstein and Fermi-Dirac distributions by non-equilibrium distributions (Wigner functions)  $f_B(x, p)$  and  $f_F(x, p)$  which depend on the space-time coordinate and the four momenta [21]. Equations (6) and (7) remain valid for bare propagators, with the equilibrium distribution functions ( $n_B, n_F$ ) replaced by the non-equilibrium ones ( $f_B, f_F$ ), but the last equations in each of (6) and (7), (i.e. the fluctuation-dissipation theorem which reflects the KMS condition), no longer hold for full propagators [28].

Equations (30) give the spectral representations of the seven 4-point functions (10) in equilibrium. These expressions remain valid out of equilibrium since the KMS condition was not used in their derivation. Out of equilibrium there are eight more 4-point vertex functions ( $G_{arr}, G_{rarr}, G_{rrar}, G_{rrra}, G_{arar}, G_{aarr}, G_{arra}$  and  $G_{rrrr}$ ) with similar spectral representations. They can be derived using the same methods as those given in Sec. III.

The results in Secs. IV and V can be generalized to non-equilibrium situations by simply replacing in (44) and (48) the Bose-Einstein and Fermi-Dirac distributions  $n_B(p^0)$  and  $n_F(p^0)$  by non-equilibrium Wigner functions  $f_B(x, p)$  and  $f_F(x, p)$ . The thermal mass  $m_\beta$  in (44) and the factors  $c_\beta, d_\beta$  in (48) become functions of  $x, m(x), c(x), d(x)$ , and it is only in the special case of thermal equilibrium that  $c = 0$  as obtained in (49). These generalized results correspond to the "hard loop" (HL) approximation in slightly off-equilibrium plasmas and are applicable in the situations discussed at the beginning of this section. We have shown that the 7 components of the 4-point function given in (10) correspond to 5 spectral densities which degenerate in the HL approximation to a single real function. This result remains valid out of equilibrium, where the KMS conditions do not hold. The eight additional 4-point functions which must be included out of equilibrium will involve more spectral functions, but in the HL approximation it is straightforward to show that they degenerate to the same HTL spectral density (55), with the thermal mass  $m_\beta$  replaced by the generalized mass  $m(x)$ .

The one-loop Ward identities in Sec. VI were obtained without explicitly doing any momentum integrals; the result thus holds independently of the form of the distribution functions (which enter through the functions  $f_i, \bar{f}_i$  in (65) and (66)). Out of equilibrium there will be additional Ward identities for the eight additional vertex functions which can be derived in the same way. For example, the Ward identities that correspond to the three functions  $G_{aarr}, G_{arra}, G_{arar}$  have been calculated, and they have the same form as those obtained in (69 e,f,g).

## VIII. CONCLUSIONS

We have studied the 4-point vertex functions in the Keldysh formulation of real-time thermal field theory [22]. This formalism has recently gained increased popularity because it avoids the need for analytical continuation associated with the imaginary time formalism, and it allows for a generalization to non-equilibrium situations. Starting from the largest time and smallest time equations which relate the 16 components of the 4-point real-time vertex function, we have derived spectral integral representations for the 7 retarded-advanced 4-point functions (10). We have explicitly calculated these 7 functions for hot QED at 1-loop order in the HTL approximation, using the Keldysh representation. In particular, we have demonstrated the usefulness of this representation for the calculation of many-point functions and showed how terms with high powers of the distribution functions cancel explicitly before any momentum integrations are done. The fully retarded vertex functions are found to be linear in the distribution functions [27]. In the HTL approximation, they have the same structure as their QCD counterparts which were derived in the ITF [4,30] as well as from kinetic theory [10]. We have also calculated the three mixed retarded-advanced 4-point functions which are needed for a complete description of the real-time 4-point vertex and which have not previously appeared in the literature. They are quadratic in the distribution functions. One of them ( $G_{rraa}$ ) was found to vanish in thermal equilibrium, while the other 4-point functions are all proportional to  $T^2$ .

We have derived spectral integral representations for the 7 retarded-advanced 4-point functions (10). The spectral densities were calculated explicitly for hot QED in the HTL approximation and found in this case to degenerate to a single real spectral function. Its trace over the Lorentz indices vanishes, and it is transverse with respect to all 4 external momenta. It obeys a simple sum rule with the correspondingly approximated 3-point spectral density.

By contracting the 7 retarded-advanced 4-point functions (10) for QED in the HTL approximation with one of the photon momenta we have derived one-loop Ward identities. This calculation was done without doing any momentum integrations, by comparing the integrands of the contracted HTL 4-point vertices with those of the HTL 3-point vertices. The resulting set of real-time Ward identities at finite temperature generalizes the zero temperature Ward identity and can be compared with the HTL Ward identity from the ITF and from kinetic theory. Due to the matrix form of the real-time thermal Green functions, the Ward identities have a more complex structure: one finds a whole class of finite temperature Ward identities which relate retarded-advanced 4-point functions to retarded-advanced 3-point vertex functions. If either the ingoing or the outgoing fermion leg has the largest time, the Ward identity involves only one kind of retarded-advanced 3-point vertex functions, and the right hand side vanishes when the contracted photon momentum ( $P_3$ ) goes to zero. If one of the photon legs has the largest time, two different retarded-advanced 3-point functions are involved, and the right hand side no longer vanishes (Eqs. (69c-f)); the corresponding component of the 4-point vertex is thus singular in the zero-momentum limit  $P_3 \rightarrow 0$  [31]. Similar features were found for the Ward identities relating the HTL 3- and 2-point functions in hot QED [20].

Our Ward identities are not general, in the sense that they were not directly derived by functional methods from the RTF path integral. However, in the case of the 3-point functions it is known that the one-HTL Ward identities [20] are identical in structure with those satisfied by the exact vertex functions [32]. We therefore expect the same to be true in the present case.

Finally, we have discussed the generalization of our results to certain classes of “moderately non-equilibrium” situations (Sec. VII) in which a generalized HTL approximation (“hard loop approximation”) can be applied. Out of equilibrium the number of independent 4-point functions is larger, but in the HL approximation the spectral functions have the same structure as in equilibrium. All of the nice features of equilibrium HTLs persist in such “moderately non-equilibrium” situations.

## ACKNOWLEDGMENTS

We are grateful for interesting discussions with M. Thoma. This work was supported by the National Natural Science Foundation of China (NSFC), the Deutsche Forschungsgemeinschaft (DFG), the Bundesministerium für Bildung und Forschung (BMBF), the Gesellschaft für Schwerionenforschung (GSI), and the Natural Sciences and Engineering and Research Council of Canada (NSERC).

- 
- [1] N.P. Landsman and Ch.G. van Weert, Phys. Rep. **145**, 141 (1987).
  - [2] J.I. Kapusta, *Finite Temperature Field Theory* (Cambridge University Press, 1989).
  - [3] M. LeBellac, *Thermal Field Theory* (Cambridge University Press, 1996).
  - [4] E. Braaten and R.D. Pisarski, Nucl. Phys. **B337**, 569 (1990); and **B339**, 310 (1990).
  - [5] M.H. Thoma, in *Quark-Gluon Plasma 2*, p. 51, ed. by R.C. Hwa (World Scientific, Singapore, 1996).
  - [6] U. Heinz, Ann. Phys. (N.Y.) **168**, 48 (1986).
  - [7] J. Frenkel and J.C. Taylor, Nucl. Phys. **B334**, 199 (1990).
  - [8] E. Braaten and R.D. Pisarski, Phys. Rev. D **45**, 1827 (1992).
  - [9] R. Jackiw, V.P. Nair, Phys. Rev. D **48**, 4991 (1993).
  - [10] J.-P. Blaizot and E. Iancu, Phys. Rev. Lett. **70**, 3376 (1993); Nucl. Phys. **B417**, 608 (1994).
  - [11] P.F. Kelly, Q. Liu, C. Lucchesi, and C. Manuel, Phys. Rev. Lett. **72**, 3461 (1994).
  - [12] S. Jeon, Phys. Rev. D **47**, 4586 (1993); and **52**, 3591 (1995).
  - [13] E. Wang, U. Heinz, and X.-F. Zhang, Phys. Rev. D **53**, 5978 (1996).
  - [14] R. Kobes and G.W. Semenoff, Nucl. Phys. **B260**, 714 (1985); and **B272**, 329 (1986).
  - [15] R. Kobes, Phys. Rev. D **43**, 1269 (1991).
  - [16] T.S. Evans, Phys. Lett. B **249**, 286 (1990); **252**, 108 (1990); and Nucl. Phys. **B374**, 340 (1992).
  - [17] J.C. Taylor, Phys. Rev. D **47** (1993) 725
  - [18] J.C. Taylor, Phys. Rev. D **48**, 958 (1993).
  - [19] M.E. Carrington and U. Heinz, Eur. Phys. J. **C1**, 619 (1998).
  - [20] Hou Defu and U. Heinz, Eur. Phys. J. **C4**, 129 (1998); and **C7**, 101 (1999).
  - [21] K.-C. Chou, Z.-B. Su, B.-L. Hao, and L. Yu, Phys. Rep. **118**, 1 (1985).
  - [22] L.V. Keldysh, Zh. Eksp. Teor. Fiz. **47**, 1515 (1964) [JETP **20**, 1018 (1965)].
  - [23] P.A. Henning, Phys. Rep. **253**, 235 (1995).

- [24] R. Kobes, Phys. Rev. D **42**, 562 (1990).
- [25] E. Wang and U. Heinz, hep-th/9809016.
- [26] Hou Defu, E. Wang, and U. Heinz, J. Phys. G **24**, 1861 (1998).
- [27] R. Baier, B. Pire, and D. Schiff, Z. Phys. C **51**, 581 (1991); P. Aurenche, E. Petitgirard and T.R. Gaztelurrutia, Phys. Lett. B **297**, 337 (1992).
- [28] M. Carrington, Hou Defu, and M.H. Thoma, Phys. Rev. D **58**, 085025 (1998); Eur. Phys. J. **C7**, 347 (1999).
- [29] J.C. Ward, Phys. Rev. **77**, 293 (1950); Y. Takahashi, Nuovo Cimento **6**, 340 (1957).
- [30] J. Frenkel and J.C. Taylor, Nucl. Phys. B **374**, 156 (1992).
- [31] We thank D. Boyanovsky and S.-Y. Wang for pointing this out. They observed that at  $p=p'$  the r.h.s. of the Ward identity (39c) in the second reference [20] develops a pinch singularity as can be seen from Eq. (38b) in the same paper. Its physical interpretation is unclear to us.
- [32] J.C. D'Olivo, M. Torres, and E. Tútuti, Phys. Rev. D **55**, 3859 (1997).